



Received 2 September 2024

Accepted 29 September 2024

Edited by K. V. Domasevitch, National Taras
Shevchenko University of Kyiv, Ukraine**Keywords:** crystal structure; 1*H*-indole;
benzenesulfonamide; π - π interactions;
hydrogen bonding; Hirshfeld surface analysis.**CCDC references:** 2387808; 2350346**Supporting information:** this article has
supporting information at journals.iucr.org/e

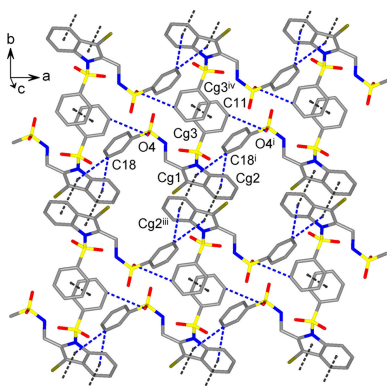
The crystal structures determination and Hirshfeld surface analysis of *N*-(4-bromo-3-methoxyphenyl)- and *N*-[[3-bromo-1-(phenylsulfonyl)-1*H*-indol-2-yl]-methyl]- derivatives of *N*-[[3-bromo-1-(phenylsulfonyl)-1*H*-indol-2-yl]methyl]benzenesulfonamide

S. Madhan,^a M. NizamMohideen,^{a*} Vinayagam Pavunkumar^b and Arasambattu K. MohanaKrishnan^b^aDepartment of Physics, The New College, Chennai 600 014, University of Madras, Tamil Nadu, India, and ^bDepartment of Organic Chemistry, University of Madras, Guindy Campus, Chennai-600 025, Tamilnadu, India. *Correspondence e-mail: mnizam.new@gmail.com

Two new phenylsulfonylindole derivatives, namely, *N*-[[3-bromo-1-(phenylsulfonyl)-1*H*-indol-2-yl]methyl]-*N*-(4-bromo-3-methoxyphenyl)benzenesulfonamide, C₂₈H₂₂Br₂N₂O₅S₂, (**I**), and *N,N*-bis[[3-bromo-1-(phenylsulfonyl)-1*H*-indol-2-yl]methyl]benzenesulfonamide, C₃₆H₂₇Br₂N₃O₆S₃, (**II**), reveal the impact of intramolecular π - π interactions of the indole moieties as a factor not only governing the conformation of *N,N*-bis(1*H*-indol-2-yl)methylamines, but also significantly influencing the crystal patterns. For **I**, the crystal packing is dominated by C-H... π and π - π bonding, with a particular significance of mutual indole-indole interactions. In the case of **II**, the molecules adopt short intramolecular π - π interactions between two nearly parallel indole ring systems [with the centroids of their pyrrole rings separated by 3.267 (2) Å] accompanied by a set of forced Br...O contacts. This provides suppression of similar interactions between the molecules, while the importance of weak C-H...O hydrogen bonding to the packing naturally increases. Short contacts of the latter type [C...O = 3.389 (6) Å] assemble pairs of molecules into centrosymmetric dimers with a cyclic $R_2^2(13)$ ring motif. These findings are consistent with the results of a Hirshfeld surface analysis and together they suggest a tool for modulating the supramolecular behavior of phenylsulfonylated indoles.

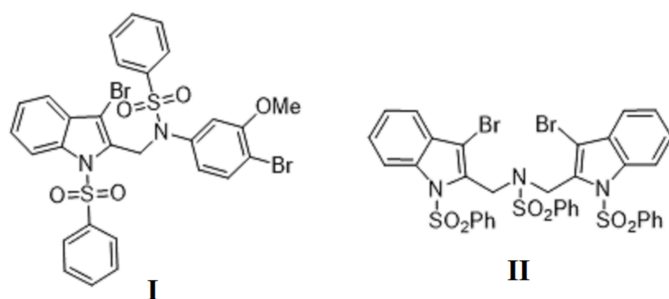
1. Chemical context

Sulfonamide derivatives found applications in modern medicine to control diseases caused by bacterial infections (Brown, 1971; Zhao *et al.*, 2016). These species have been famous as sulfa drugs for over 70 years since the discovery of their activity. They are still used as antibiotics (Gulcin & Taslimi, 2018), in spite of the later introduction of penicillin. In particular, numerous formulations based on sulfonamides have repeatedly been used as chemotherapeutics for their antibacterial (Ovung & Bhattacharyya, 2021; Badr, 2008), antifungal (Hanafy *et al.*, 2007) and hypoglycemic properties (Chohan *et al.*, 2010; El-Sayed *et al.*, 2011). Among drugs of other types, sulfonamides also display appreciable antitumor, anticancer, and antithyroid activities (Scozzafava *et al.*, 2003). Some sulfonamide products also possess carbonic anhydrases (CA) inhibition properties (Suparan *et al.*, 2001). The production of new compounds with noteworthy biological activity, which are suited as antiviral and antimicrobial agents, drives interest in synthetic approaches for sulfonamide-functionalized heterocyclic ring systems (Azzam *et al.*, 2020).



Published under a CC BY 4.0 licence

Identifying the significance of such compounds for biochemical uses and drug discovery, and our continuing study of the development of indole products have prompted us to examine a series of corresponding *N*-sulfonyl- and bromo-substituted species. The need for deeper functionalization of the systems by introducing bromine substitutes is motivated by the fact that the presence of halogen atoms in molecules commonly enhances various biological activities and thus halogenation may be recognized as an essential tool for drug optimization (Murphy *et al.*, 2003). For example, the occurrence of bromine atoms on a phenol ring is important for improved antimicrobial activity (Bouthenet *et al.*, 2011). Structural trends in such compounds, including subtle features of their intermolecular interactions, could be applicable to the specific targeting of the substrates in biomedical systems and therefore they may provide new insights into the action of sulfonamide derivatives. In particular, Adson & Grant (2001) categorized the hydrogen-bonding preferences of sulfonamides. The availability of multiple aromatic groups in *N*-sulfonylated indoles imposes also possibility for versatile stacking patterns, which may be competitive to conventional hydrogen bonding. We report herein the crystal-structure determination and Hirshfeld surface analysis of two new indoles: namely, *N*-[[3-bromo-1-(phenylsulfonyl)-1*H*-indol-2-yl]methyl]-*N*-(4-bromo-3-methoxyphenyl)benzenesulfonamide, $C_{28}H_{22}Br_2N_2O_5S_2$, (**I**), and *N,N*-bis[[3-bromo-1-(phenylsulfonyl)-1*H*-indol-2-yl]methyl]benzenesulfonamide, $C_{36}H_{27}Br_2N_3O_6S_3$, (**II**), which feature a complex interplay of weak hydrogen-bonding and π - π interactions.



2. Structural commentary

The molecular structures of the title compounds, which differ in substituents at the phenylsulfonylated exocyclic N2 atoms (*N*-(4-bromo-3-methoxyphenyl) for **I** and *N*-[[3-bromo-1-(phenylsulfonyl)-1*H*-indol-2-yl]methyl] for **II**), are illustrated in Figs. 1 and 2, respectively. In both the cases, the indole ring systems (N1/C1–C8 and N3/C23–C30) are essentially planar, with a maximum deviation from the corresponding mean planes of 0.039 (4) Å observed for C8 atom in **II**. The torsion angles involving the sulfonamide fragments, O2–S1–N1–C1 [–152.6 (3) for **I** and –175.2 (3)° for **II**], O3–S2–C16–C17 [–153.9 (3) for **I** and –146.4 (3)° for **II**] and O5–S3–N3–C23 [–178.7 (3)° for **II**] indicate an anti-periplanar conformation of the sulfonyl moiety. The dihedral angle between sulfonyl-bound phenyl rings (C9–C14) and the carrier indole ring systems (N1/C1–C8) are 62.0 (2)° for **I** and

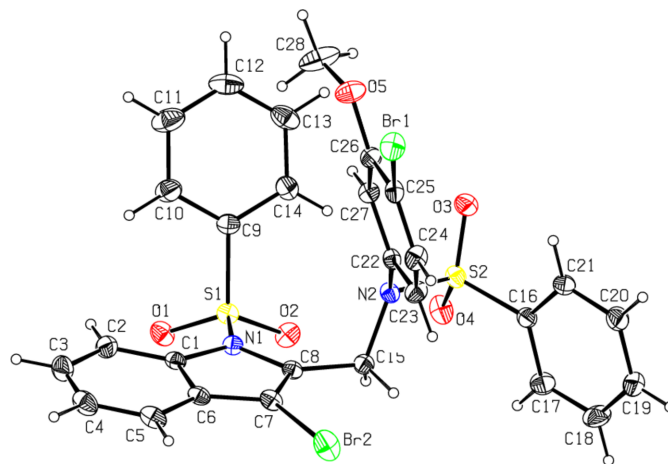


Figure 1

The molecular structure of compound **I**, with atom labeling and displacement ellipsoids drawn at the 20% probability level.

70.9 (2)° for **II**, unlike the orthogonal orientation of these groups in previously reported *N*-phenylsulfonyl indoles (Madhan *et al.*, 2022, 2023*a,b*, 2024*a,b*). In **I**, the dihedral angle between two sulfonyl-bound phenyl rings (C9–C14 and C16–C21) is 59.0 (2)°, while in **II** they are nearly orthogonal [86.5 (2)°]. The methoxy-bound phenyl ring (C22–C27) in **I** is

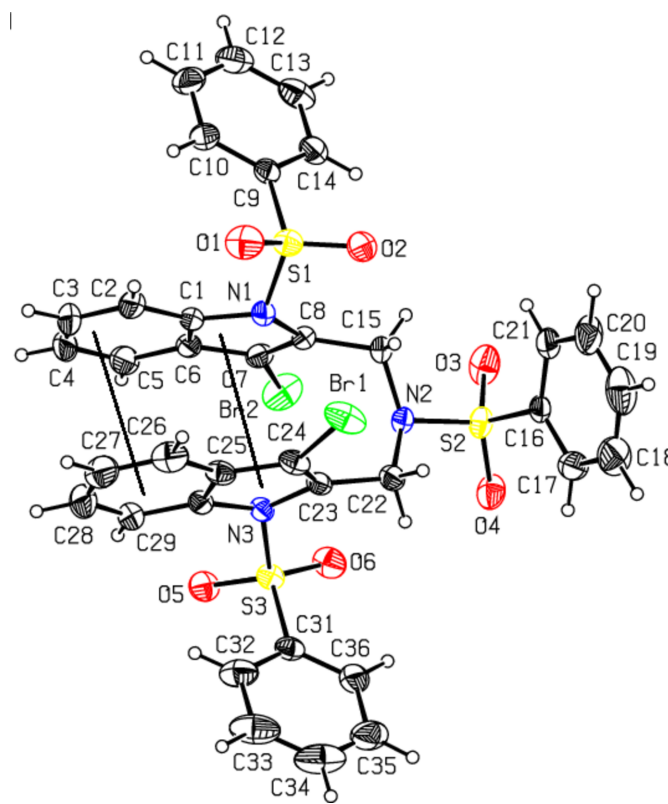


Figure 2

The molecular structure of compound **II**, with atom labeling and displacement ellipsoids drawn at the 30% probability level. The dashed lines indicate the intramolecular π - π interactions of the indole ring systems.

Table 1
Hydrogen-bond geometry (Å, °) for **I**.

<i>D</i> – <i>H</i> ··· <i>A</i>	<i>D</i> – <i>H</i>	<i>H</i> ··· <i>A</i>	<i>D</i> ··· <i>A</i>	<i>D</i> – <i>H</i> ··· <i>A</i>
C2–H2···O1	0.93	2.39	2.908 (5)	115
C11–H11···O4 ⁱ	0.93	2.76	3.503 (6)	137
C15–H15 <i>B</i> ···O2	0.97	2.31	2.886 (4)	117
C18–H18···Cg(N1/C1/C6–C8) ⁱⁱⁱ	0.93	2.99	3.861 (8)	156
C18–H18···Cg(C1–C6) ⁱⁱ	0.93	2.81	3.579 (1)	141

Symmetry codes: (i) $x + 1, y, z$; (ii) $x - 1, y, z$.

also inclined to the indole framework, subtending a dihedral angle of 73.23 (1)°.

The geometric parameters of **I** and **II** agree well with those reported for related structures (Madhan *et al.*, 2022, 2023*a,b*, 2024*a,b*). The sulfonamide S atoms exhibit a distorted tetrahedral geometry with the O–S–O angles lying in the range of 119.9 (2)–120.3 (2)°. The increase in these angles, accompanied by a simultaneous decrease in the N–S–C angles [which are 104.3 (2)–106.1 (2)°], from the ideal tetrahedral values are attributed to the Thorpe–Ingold effect (Bassindale, 1984). The widening of the angles may be due to the repulsive interaction between the two short S=O bonds. In both compounds, the expansion of the *ipso* angles at atoms C1, C3, C4 (and C25, C27, C28 in **II**), together with the contraction of the apical angles at atoms C2, C5, C6 (and C26, C29, C30 in **II**) are caused by fusion of the smaller pyrrole ring with the six-membered benzene ring and the strain is taken up by the angular distortion rather than by bond-length distortion (Allen, 1981).

The molecular conformation of compound **I** is stabilized by the weak intramolecular hydrogen bond C2–H2···O1 [C2···O1 = 2.908 (5) Å] formed by the sulfone O atoms, which generates an *S*(6) ring motif. The similar interaction in compound **II** [C2···O1 = 2.993 (7) Å] is accompanied by three additional intramolecular hydrogen bonds involving methylene donors and sulfone acceptors [C15···O2 = 2.850 (5) Å, C22···O6 = 2.950 (5) Å and C29···O5 = 2.907 (5) Å], which generate *S*(6) ring motifs.

The most striking feature of the molecular structures is the specific conformation of **II**, which is controlled by an intramolecular π – π interaction between the two indole ring systems (Fig. 2). Their planes are almost parallel, while adopting a small angle of 7.2 (2)°. Two pyrrole and two benzene rings are situated one on the top of another, with the corresponding intercentroid distances being 3.267 (5) and 3.593 (5) Å, respectively, and with the shortest contact of 3.035 (5) Å observed between atoms C8 and C23. A similar intramolecular pairing of aromatic rings separated by flexible triatomic spacers is relevant for the appropriate model of dibenzylketone (Lima *et al.*, 2010). For the latter, the stacked conformation was associated with a relatively small stabilizing enthalpic effect of about 12.9 kJ mol^{–1} and therefore the crystal structure did not inherit the intramolecular stacking observed for the gas phase and solution structures. In contrary, the energetics of the intramolecular indole–indole interaction could be estimated to be far superior (up to 50–60 kJ mol^{–1}; Madhan *et al.*, 2024*a*) due to the significantly larger interaction areas and higher contribution of London dispersion forces.

Table 2
Hydrogen-bond geometry (Å, °) for **II**.

<i>D</i> – <i>H</i> ··· <i>A</i>	<i>D</i> – <i>H</i>	<i>H</i> ··· <i>A</i>	<i>D</i> ··· <i>A</i>	<i>D</i> – <i>H</i> ··· <i>A</i>
C2–H2···O1	0.93	2.43	2.993 (7)	119
C13–H13···O3 ⁱ	0.93	2.80	3.324 (6)	117
C14–H14···O4 ⁱ	0.93	2.78	3.558 (5)	142
C15–H15 <i>B</i> ···O2	0.97	2.25	2.850 (5)	119
C18–H18···O3 ⁱⁱⁱ	0.93	2.73	3.575 (6)	151
C19–H19···O4 ⁱⁱⁱ	0.93	2.59	3.443 (6)	152
C19–H19···O6 ⁱⁱⁱ	0.93	2.81	3.467 (6)	129
C20–H20···Br2 ⁱⁱⁱ	0.93	3.02	3.536 (5)	117
C22–H22 <i>A</i> ···O6	0.97	2.39	2.950 (5)	116
C27–H27···O1 ^{iv}	0.93	2.48	3.389 (6)	164
C28–H28···O5 ^v	0.93	2.63	3.547 (6)	170
C29–H29···O5	0.93	2.35	2.907 (5)	118
C34–H34···O3 ⁱⁱ	0.93	2.62	3.360 (6)	137
C35–H35···Cg(C16–C21) ^{vi}	0.93	2.91	3.729 (7)	147

Symmetry codes: (i) $x - \frac{1}{2}, -y + \frac{1}{2}, z - \frac{1}{2}$; (ii) $x + 1, y, z$; (iii) $x + \frac{1}{2}, -y + \frac{1}{2}, z - \frac{1}{2}$; (iv) $-x + 1, -y + 1, -z + 1$; (v) $-x + 1, -y + 1, -z + 2$; (vi) $x - \frac{1}{2}, -y - \frac{1}{2}, z - \frac{1}{2}$.

The impact of the resulting intramolecular stacking on the sulfonylindole geometry is visible from the inspection of configuration around sulfonyl N atoms. The sum of the bond angles around N1 in **I** [359.5 (2)°] indicates *sp*² hybridization (Beddoes *et al.*, 1986). However, in the case of **II**, two such parameters are essentially smaller [346.6 (2)° and 349.9 (2)°, for N1 and N3, respectively] and therefore these indole N atoms are pyramidalized to almost the same extent as the exocyclic sulfonamide N2 atoms [347.8 (2)° in **I** and 342.2 (2)° in **II**]. The configuration for the latter is typical for sulfonamides, which lack π -bonding between the N and S atoms (Blahun *et al.*, 2020). The perceptible pyramidalization of the indole N atoms may be viewed as a consequence of the steric strain imposed by close contacts between the Br and O atoms of two stacked indole systems [the shortest contact is Br2···O6 = 3.592 (4) Å]. At the same time, as a result of the electron-withdrawing character of the phenylsulfonyl group, the indole N–C*sp*² bond lengths [N1–C1 = 1.415 (4) and N1–C8 = 1.427 (4) Å in **I**; 1.427 (5)–1.430 (4) Å in **II**] are longer than the mean value of 1.355 (14) Å for this bond (Allen *et al.*, 1987; Cambridge Structural Database (CSD), Version 5.37; Groom *et al.*, 2016).

3. Supramolecular features

With the absence of conventional hydrogen-bond donor functionality, the supramolecular patterns of both compounds are controlled by weaker interactions, namely by weak C–H···O, C–H···Br and C–H··· π hydrogen bonds (Tables 1 and 2) and slipped π – π stacking interactions (Table 3). In the case of **I**, the latter is prevalent. Antiparallel stacking of two inversion-related indole ring systems [symmetry code: (iii) $-x + 1, -y + 1, -z + 1$] assemble the molecules into dimers, which are connected into chains along the *b*-axis direction by means of π – π interactions between inversion-related phenyl rings [symmetry code: (iv) $-x + 1, -y + 2, -z + 1$] (Fig. 3). For the indole–indole interaction, the corresponding intercentroid distances of 3.532 (2) Å and shortest contacts, down to 3.456 (2) Å (Table 3), are consistent well with those for π – π interactions seen in the crystal structures of similar

Table 3
Geometry of stacking interactions (Å, °) for **I** and **II**.

C_g is a group centroid; $\text{plane} \cdots C_g B$ is the distance between the mean plane of group A and the centroid of interacting group B ; ipa is the interplanar angle; sa is the slippage angle, which is the angle of the $C_g A \cdots C_g B$ axis to the group A mean plane normal.

Compound	Group A	Group B	Shortest contact	$C_g A \cdots C_g B$	Plane $\cdots C_g B$	ipa	sa
I	(N1/C1/C6–C8)	(C1–C6) ⁱⁱⁱ	3.456 (2)	3.532 (2)	3.450 (2)	1.2 (2)	12.4 (2)
	(C9–C14)	(C9–C14) ^{iv}	3.397 (2)	3.824 (2)	3.397 (2)	0	27.3 (2)
II	(N1/C1/C6–C8)	(N3/C30/C23–C25)	3.225 (2)	3.267 (2)	3.256 (2)	10.4 (3)	4.8 (2)
	(C1–C6)	(C25–C30)	3.499 (2)	3.593 (3)	3.531 (2)	4.9 (3)	10.7 (2)
	(C9–C14)	(C31–C36) ^{vii}	3.464 (2)	3.952 (3)	3.636 (2)	6.64 (16)	23.0 (2)

Symmetry codes for **I**: (iii) $-x + 1, -y + 1, -z + 1$; (iv) $-x + 1, -y + 2, -z + 1$; for **II**: (vii) $x - 1, y, z - 1$.

1-(phenylsulfonyl)-1*H*-indole derivatives (Madhan *et al.*, 2024*a*). Further connection of the chains by C–H $\cdots \pi$ hydrogen bonds yields corrugated layers parallel to the ab plane. Two such C–H $\cdots \pi$ interactions actualize above and below the indole-indole stacks and they are bifurcated, involving both benzo- and pyrrole rings as the acceptors. The corresponding separations are $C18 \cdots C_g(N1/C1/C6-C8)^{ii} =$

3.861 (8) Å and $C18 \cdots C_g(C1-C6)^{ii} = 3.579$ (1) Å [symmetry code: (ii) $x - 1, y, z$]. The only C–H $\cdots O$ bond in the structure [$C11 \cdots O4^i = 3.503$ (6) Å; symmetry code: (i) $x + 1, y, z$] is also identified withing this layer.

One can note that in **I**, and also in other comparable 1-(phenylsulfonyl)-1*H*-indoles (Madhan *et al.*, 2024*a*), the favorable π – π bonded duo is generated due to the interactions at only one axial side of the indole ring system. Therefore, in the case of **II**, the intermolecular π – π interactions of the latter are completely suppressed due to the generation of the intramolecular indole–indole stack. This is in line with the increased significance of C–H $\cdots O$ interactions in the crystal of **II**. The shortest hydrogen-bond contacts are observed for sulfonic O-atom acceptors [$C27 \cdots O1^{iv} = 3.389$ (6) Å; symmetry code: (iv) $-x + 1, -y + 1, -z + 1$]. These bonds assemble pairs of the molecules into centrosymmetric dimers (Fig. 4) with a cyclic $R_2^2(13)$ (Bernstein *et al.*, 1995) ring motif. The dimers are further integrated into a three-dimensional framework. The amino-bound phenylsulfonyl groups are held together by a set of C–H $\cdots O$ bonds [*viz.* $C18 \cdots O3^{ii} = 3.575$ (6) and $C19 \cdots O4^{iii} = 3.443$ (6) Å; symmetry codes: (ii) $x + 1, y, z$; (iii) $x + \frac{1}{2}, -y + \frac{1}{2}, z - \frac{1}{2}$] and constitute their own layer connectivities in the form of flat square nets, which are parallel to the ac plane (Fig. 4*b*). These layers are separated by 17.39 Å, which is half of the b -axis parameter of the unit cell, and are linked *via* bis(indolemethyl)amine fragments of the above dimers (Fig. 4*b*). These bis(indolemethyl)amine fragments themselves afford nominal layers with a set of weak intermolecular interactions, such as C–H $\cdots O$ bonds [$C34 \cdots O5^{ii} = 3.360$ (6) Å; symmetry code: (ii) $x + 1, y, z$] and relatively distal π – π interactions between the outer phenyl rings, with an intercentroid distance of 3.952 (3) Å (Fig. 4*c*).

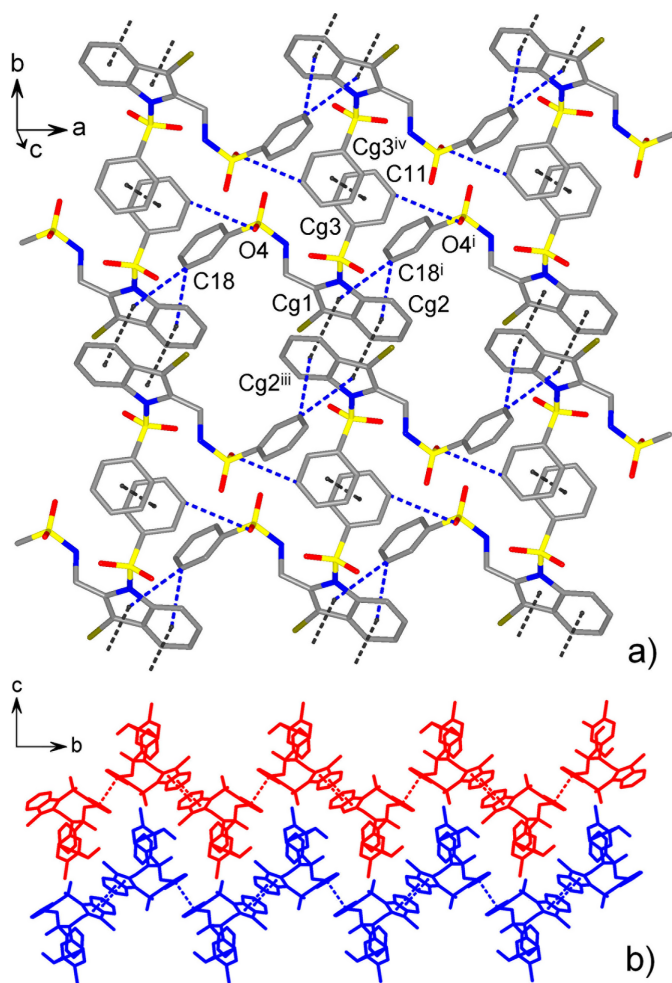
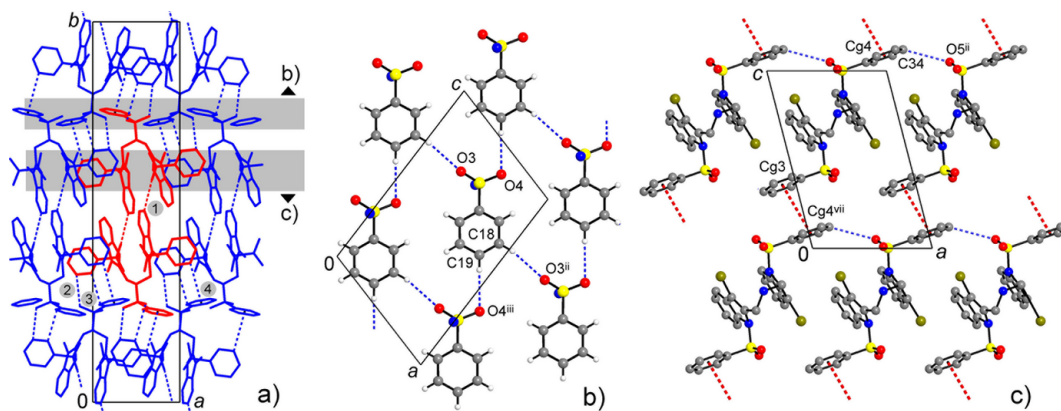


Figure 3
(*a*) Crystal packing of compound **I**, viewed in a projection nearly on the ab plane, showing a non-covalent layer assembled by π – π and C–H $\cdots O$ interactions (identified by dotted lines). (*b*) Packing of two successive corrugated layers. [Symmetry codes: (i) $x + 1, y, z$; (iii) $-x + 1, -y + 1, -z + 1$; (iv) $-x + 1, -y + 2, -z + 1$.]

4. Hirshfeld surface analysis

In order to investigate the weak intermolecular interactions in the crystal, the Hirshfeld surfaces (d_{norm} , curvedness and shape-index) and 2D fingerprint plots were generated using *Crystal Explorer 17.5* (Spackman *et al.*, 2021). The d_{norm} mapping uses the normalized functions of d_i and d_e (Fig. 5), with white surfaces indicating contacts with distances equal to the sum of van der Waals (vdW) radii, while red and blue colors reflect contacts at the distances below and above sum of the corresponding vdW radii, respectively.


Figure 4

(a) Projection of the structure of **II** on the *ab* plane, showing the assembly of centrosymmetric C–H...O-bonded dimers and their integration into the three-dimensional framework. An individual dimer is colored red and its principal interactions C27–H...O1^{iv}, C13–H...O3ⁱ, C14–H...O4ⁱ and C35–H...Cg(C16–C21)^{vi} are labeled as 1–4, respectively. Two subconnectivities, which are orthogonal to the drawing plane, are marked with gray strips and they are detailed in the projections on the *ac* plane: (b) phenylsulfonyl layer; (c) π – π and C–H...O interactions between the molecules of **II**. [Symmetry codes: (i) $x - \frac{1}{2}, -y + \frac{1}{2}, z - \frac{1}{2}$; (ii) $x + 1, y, z$; (iii) $x + \frac{1}{2}, -y + \frac{1}{2}, z - \frac{1}{2}$; (iv) $-x + 1, -y + 1, -z + 1$; (vi) $x - \frac{1}{2}, -y - \frac{1}{2}, z - \frac{1}{2}$; (vii) $x - 1, y, z - 1$.]

The Hirshfeld surfaces for two compounds mapped over d_{norm} using a fixed color scale of -0.125 (red) to 1.678 a.u. (blue) for **I** and -0.198 (red) to 1.491 a.u. (blue) for **II** are shown in Fig. 5. One can note weakness of intermolecular bonding in a system that is, particularly the case of **I**, showing preferably normal van der Waals separations (denoted with several white regions on the surface). The only identified pair of diffuse red spots corresponds to C–H...O bonds. In the case of **II**, the observed low intense and diffuse red spots are slightly larger in number, which supports the increased significance of weak hydrogen-bonding interactions. The electrostatic potential was also mapped on the Hirshfeld surface using a STO-3G basis set and the Hartree–Fock level of theory (Spackman & Jayatilaka, 2009). The C–H...O hydrogen-bond donors and acceptors are shown as blue and red regions around the atoms corresponding to positive and negative electrostatic potentials, respectively (Fig. 6a). The presence of π – π stacking interactions is indicated by red and blue triangles on the shape-index surface (Fig. 6b). Areas on the Hirshfeld surface with high curvedness tend to divide the surface into contact patches with each neighboring molecule. The coordination number in the crystal is defined by the curvedness of the Hirshfeld surface (Fig. 6c). The nearest neighbor in the coordination environment of a molecule is

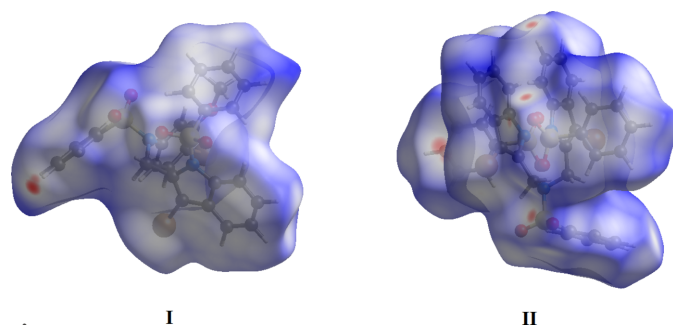


Figure 5
The Hirshfeld surfaces of compounds **I** and **II** mapped over d_{norm} .

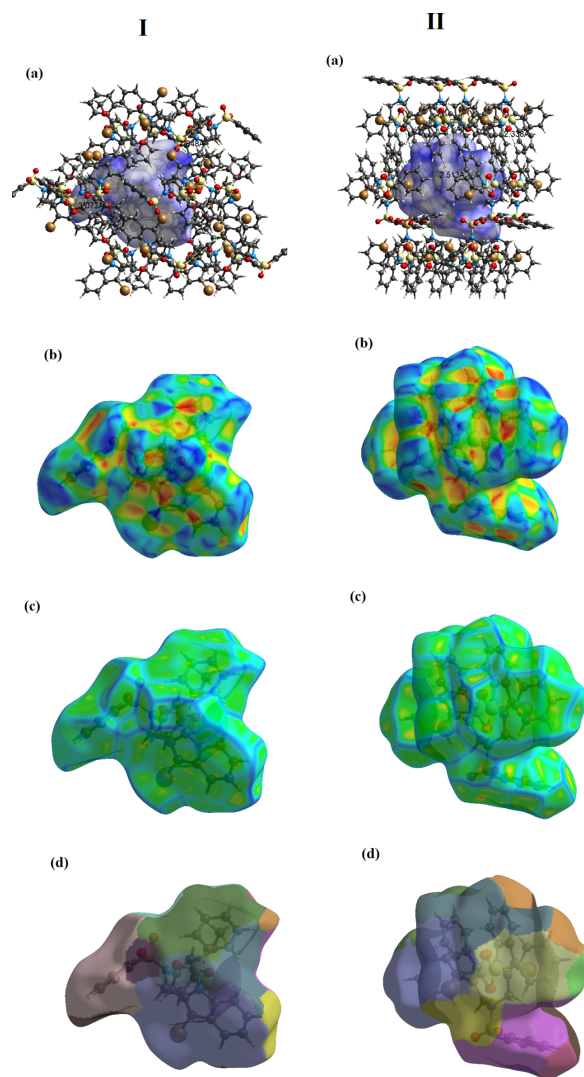
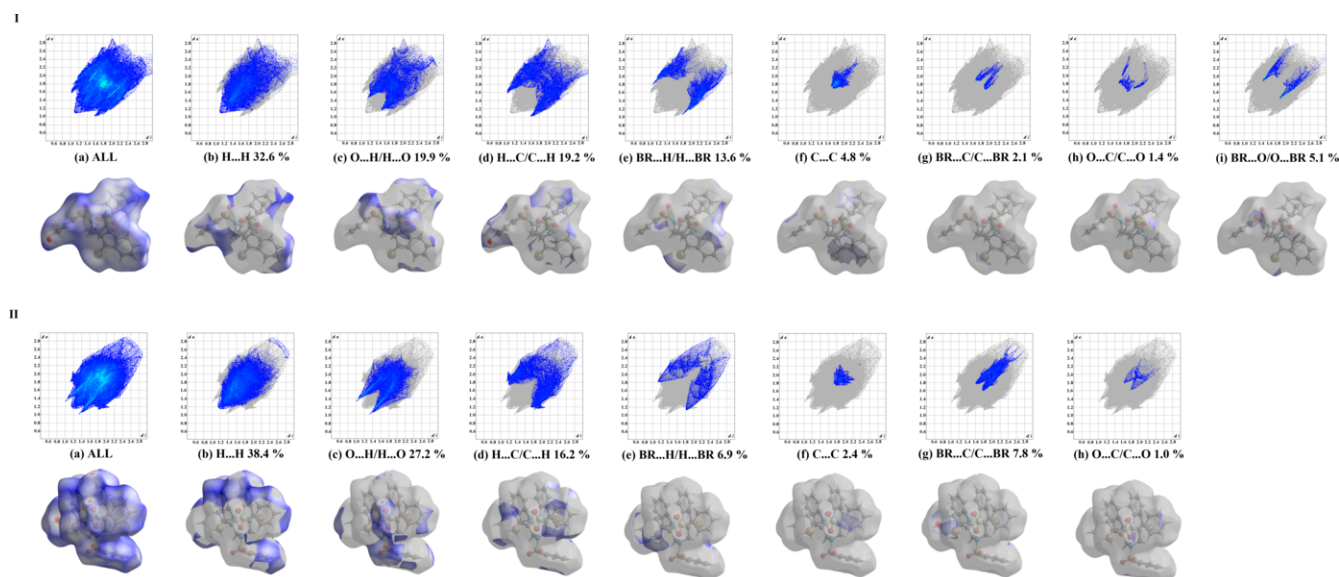


Figure 6
Hirshfeld surfaces for visualizing the intermolecular contacts of the title compounds: (a) electrostatic potential, (b) shape-index, (c) curvedness and (d) fragment patches.


Figure 7

Two-dimensional fingerprint plots for **I** and **II** for all contacts and delineated into the principal contributions of H...H, O...H/H...O, C...H/H...C, Br...H/H...Br, Br...O/O...Br, C...C, Br...C/C...Br and O...C/C...O contacts. Other contributors account for less than 1.0% of contacts to the surface areas.

identified from the color patches on the Hirshfeld surface depending on their closeness to adjacent molecules (Fig. 6*d*).

Two-dimensional fingerprint plots showing the occurrence of all intermolecular contacts (McKinnon *et al.*, 2007) are presented in Fig. 7. The plots for H...H contacts (Fig. 7*b*), which represent the largest contributions to the Hirshfeld surfaces (over 30%), show a distinct pattern with a minimum value of $d_e = d_i = 1.1$ Å. Beyond these largest fractions, the short contacts are overwhelmingly O...H/H...O (Fig. 7*c*) and C...H/H...C (Fig. 7*d*), which deliver as much as 19.9 and 19.2%, respectively, to the Hirshfeld surface in **I** and 27.2 and 16.2% in **II**. The significant increase in the O...H/H...O contributions when moving from **I** to **II** reflects the growing significance of C—H...O binding. This is in line with a larger number of the available O-atom acceptors in the latter case, but also it is a consequence of the elimination of intermolecular π – π indole bonding. Accordingly, the pair of spikes identifying O...H/H...O contacts on the plots is more diffuse in the case of **I**. We note also a suppression of Br...H/H...Br contacts (6.9% for **II** versus 13.6% for **I**). This fact does not provide a basis for comparison of the acceptor abilities of the indole- and phenyl-bound Br atoms, but rather reflects the steric unavailability of Br in **II** due to the forced intramolecular interactions with sulfonyl O atoms. It is worth mentioning that the accumulation of unfavorable Br...O/O...Br contacts within the molecule of **II** causes the elimination of such contacts between the molecules. This situation is evidenced by markedly different contributions of Br...O/O...Br contacts to the surface areas, which are 5.1% for **I**, but are completely absent in the case of **II**. An overlap between nearly parallel aromatic frames, due to the slipped π – π interactions, is clearly indicated by the C...C plots in the form of blue–green areas centered at *ca* $d_e = d_i = 1.8$ Å. A 50% decrease in the C...C contacts (2.4% for **II** versus 4.8% for **I**)

is also a consequence of intramolecular indole–indole stacking, which mitigates against similar in nature intermolecular interactions.

In brief, the Hirshfeld surface analysis confirms the importance of weak hydrogen bonding and contacts associated with the π – π interactions in establishing the packing. These results complement the main merit of the structure analysis and in total they suggest the possibility of controlling the supramolecular behavior of sulfonylated indoles as possible biomedical materials.

5. Database survey

A search of the Cambridge Structural Database (Version 5.37; Groom *et al.*, 2016) indicated 123 compounds incorporating the phenylsulfonyl-1*H*-indole moiety. Of these, the most closely related examples are provided by structures of bromosubstituted 3-methyl-1-(phenylsulfonyl)-1*H*-indole derivatives (JOMJII, JOMJAA and JOMJEE; Madhan *et al.*, 2024*b*), ethyl 2-acetoxymethyl-1-phenylsulfonyl-1*H*-indole-3-carboxylate (HUCQUS; Gunasekaran *et al.*, 2009), 3-iodo-2-methyl-1-phenylsulfonyl-1*H*-indole (ULESEK; Ramathilagam *et al.*, 2011) and 1-(2-bromomethyl-1-phenylsulfonyl-1*H*-indol-3-yl) propan-1-one (CIQFEP; Umadevi *et al.*, 2013). In these structures, the sulfonyl-bound phenyl rings are almost orthogonal to the indole ring systems, with the corresponding dihedral angles lying in the range 73.35 (7)–89.91 (11)°.

6. Synthesis and crystallization

Compound I: To a solution of *N*-(3-methoxyphenyl)-*N*-{[1-(phenylsulfonyl)-1*H*-indol-2-yl]methyl}benzenesulfonamide (0.45 g, 0.845 mmol) in 5 ml of dry CH₂Cl₂, a mixture of phenyliodonium diacetate (0.40 g, 1.268 mmol) and CuBr₂

Table 4
Experimental details.

	I	II
Crystal data		
Chemical formula	C ₂₈ H ₂₂ Br ₂ N ₂ O ₅ S ₂	C ₃₆ H ₂₇ Br ₂ N ₃ O ₆ S ₃
<i>M_r</i>	690.41	853.60
Crystal system, space group	Monoclinic, <i>P</i> ₂ ₁ / <i>n</i>	Monoclinic, <i>P</i> ₂ ₁ / <i>n</i>
Temperature (K)	303	303
<i>a</i> , <i>b</i> , <i>c</i> (Å)	9.5718 (6), 14.4498 (8), 20.0041 (12)	8.2664 (4), 34.7886 (18), 12.5972 (6)
β (°)	92.874 (2)	104.550 (2)
<i>V</i> (Å ³)	2763.3 (3)	3506.5 (3)
<i>Z</i>	4	4
Radiation type	Mo <i>K</i> α	Mo <i>K</i> α
μ (mm ⁻¹)	3.13	2.54
Crystal size (mm)	0.29 × 0.24 × 0.20	0.29 × 0.19 × 0.04
Data collection		
Diffractometer	Bruker D8 Venture Diffractometer	Bruker D8 Venture Diffractometer
Absorption correction	Multi-scan (<i>SADABS</i> ; Krause <i>et al.</i> , 2015)	Multi-scan (<i>SADABS</i> ; Krause <i>et al.</i> , 2015)
<i>T</i> _{min} , <i>T</i> _{max}	0.589, 0.753	0.491, 0.745
No. of measured, independent and observed [<i>I</i> > 2σ(<i>I</i>)] reflections	90697, 5234, 4173	73921, 6434, 5196
<i>R</i> _{int}	0.071	0.071
Refinement		
<i>R</i> [<i>F</i> ² > 2σ(<i>F</i> ²)], <i>wR</i> (<i>F</i> ²), <i>S</i>	0.040, 0.099, 1.05	0.048, 0.120, 1.12
No. of reflections	5234	6434
No. of parameters	353	451
H-atom treatment	H-atom parameters constrained	H-atom parameters constrained
Δρ _{max} , Δρ _{min} (e Å ⁻³)	1.74, -1.41	0.46, -0.47

Computer programs: *APEX2* and *SAINT* (Bruker, 2016), *SHELXT2018/2* (Sheldrick, 2015a), *SHELXL2019/2* (Sheldrick, 2015b), *ORTEP-3 for Windows* (Farrugia, 2012) and *Mercury* (Macrae *et al.*, 2020), *WinGX* (Farrugia, 2012), *pubCIF* (Westrip, 2010) and *PLATON* (Spek, 2020).

(0.56 g, 2.537 mmol) in 10 ml of CH₂Cl₂ was slowly added at 273 K. The reaction mixture was allowed to stir for 3 h at 273 K under an N₂ atmosphere. After completion of the reaction (monitored by TLC), it was poured over cooled saturated aqueous NaHCO₃ solution (20 mL) and then extracted with CH₂Cl₂ (2 × 10 mL). The extract was dried over Na₂SO₄. Removal of the solvent followed by recrystallization of the crude product from 5 mL of methanol afforded *N*-[[3-bromo-1-(phenylsulfonyl)-1*H*-indol-2-yl]methyl]-*N*-(4-bromo-3-methoxyphenyl)benzenesulfonamide (0.45 g, 78%) as a colorless solid, m.p. = 495–496 K. ¹H NMR (300 MHz, CDCl₃), δ, p.p.m.: 7.96 (*d*, *J* = 8.4 Hz, 1H), 7.69–7.64 (*m*, 4H), 7.57–7.34 (*m*, 6H), 7.29–7.24 (*m*, 2H), 7.20–7.11 (*m*, 2H), 6.36 (*s*, 1H), 6.25 (*d*, *J* = 8.4 Hz, 1H), 5.28 (*s*, 2H), 3.49 (*s*, 3H). ¹³C{¹H} NMR (75 MHz, CDCl₃), δ, p.p.m.: 155.4, 138.0, 137.9, 137.4, 136.3, 134.2, 133.1, 132.6, 130.2, 129.4, 128.8, 128.4, 128.2, 126.8, 126.6, 124.5, 122.7, 120.1, 115.2, 113.6, 111.7, 107.7, 56.1, 45.8. DEPT-135 ¹³C NMR (CDCl₃), δ, p.p.m.: 134.2, 133.1, 132.6, 129.4, 128.9, 128.2, 126.8, 126.6, 124.5, 122.7, 120.2, 115.2, 113.6, 56.1, 45.8. HRMS (ESI) *m/z*: [*M*+H]⁺ Calculated for C₂₈H₂₃⁷⁹Br₂N₂O₅S₂: 688.9415; found: 688.9407.

Compound II: To a solution of *N,N*-bis[[1-(phenylsulfonyl)-1*H*-indol-2-yl]methyl]benzenesulfonamide (0.25 g, 0.359 mmol) in 5 ml of dry CH₂Cl₂, a mixture of phenyliodonium diacetate (0.23 g, 0.719 mmol) and CuBr₂ (0.24 g, 1.079 mmol) in 10 ml of CH₂Cl₂ was slowly added at 273 K. The reaction mixture was allowed to stir for 3 h at 273 K under an N₂ atmosphere. After completion of the reaction (monitored by TLC), it was poured over cooled saturated aqueous NaHCO₃ solution (20 mL) and then extracted with CH₂Cl₂ (2

× 10 mL). The extract was dried over Na₂SO₄. Removal of the solvent followed by recrystallization of the crude product from 5 ml of methanol afforded *N,N*-bis[[3-bromo-1-(phenylsulfonyl)-1*H*-indol-2-yl]methyl]benzenesulfonamide (0.15 g, 60%) as a colorless solid, m.p. = 529–531 K. ¹H NMR (300 MHz, CDCl₃), δ, p.p.m.: 7.93 (*d*, *J* = 8.1 Hz, 2H), 7.77 (*d*, *J* = 7.5 Hz, 2H), 7.52–7.45 (*m*, 6H), 7.38–7.19 (*m*, 13H), 7.14–7.09 (*m*, 2H), 5.14 (*s*, 4H). ¹³C{¹H} NMR (75 MHz, CDCl₃), δ, p.p.m.: 138.9, 137.4, 136.6, 133.9, 131.9, 129.5, 129.2, 128.0, 127.5, 126.6, 126.3, 124.6, 120.0, 115.7, 109.2, 45.0.

7. Refinement

Crystal data, data collection and structure refinement details are summarized in Table 4. All hydrogen atoms were positioned geometrically and refined as riding with C—H = 0.93 Å (aromatic CH), 0.97 Å (CH₂) and 0.96 Å (CH₃) and 0.97 Å with *U*_{iso}(H) = 1.5*U*_{eq}(C) for methyl groups and 1.2*U*_{eq}(C) for other H atoms.

Acknowledgements

The authors are thanks to the SAIF, IIT, Madras, India, for the data collection.

References

- Adson, D. A. & Grant, D. J. W. (2001). *J. Pharm. Sci.* **90**, 2058–2077.
Allen, F. H. (1981). *Acta Cryst.* **B37**, 900–906.

- Allen, F. H., Kennard, O., Watson, D. G., Brammer, L., Orpen, A. G. & Taylor, R. (1987). *J. Chem. Soc. Perkin Trans. 2*, pp. S1–19.
- Azzam, R. A., Elgemeie, G. H. & Osman, R. R. (2020). *J. Mol. Struct.* **1201**, 127194.
- Badr, E. E. (2008). *J. Dispersion Sci. Technol.* **29**, 1143–1149.
- Bassindale, A. (1984). *The Third Dimension in Organic Chemistry*, ch. 1, p. 11. New York: John Wiley and Sons.
- Beddoes, R. L., Dalton, L., Joule, T. A., Mills, O. S., Street, J. D. & Watt, C. I. F. (1986). *J. Chem. Soc. Perkin Trans. 2*, pp. 787–797.
- Bernstein, J., Davis, R. E., Shimon, L. & Chang, N.-L. (1995). *Angew. Chem. Int. Ed. Engl.* **34**, 1555–1573.
- Blahun, O. P., Rozhenko, A. B., Rusanov, E., Zhersh, S., Tolmachev, A. A., Volochnyuk, D. M. & Grygorenko, O. O. (2020). *J. Org. Chem.* **85**, 5288–5299.
- Bouthenet, E., Oh, K.-B., Park, S., Nagi, N. K., Lee, H.-S. & Matthews, S. E. (2011). *Bioorg. Med. Chem. Lett.* **21**, 7142–7145.
- Brown, G. M. (1971). *Adv. Enzymol. Relat. Areas Mol. Biol.* **35**, 35–77.
- Bruker (2016). *APEX2 and SAINT*. Bruker AXS Inc., Madison, Wisconsin, USA.
- Chohan, Z. H., Youssoufi, M. H., Jarrahpour, A. & Ben Hadda, T. (2010). *Eur. J. Med. Chem.* **45**, 1189–1199.
- El-Sayed, N. S., El-Bendary, E. R., El-Ashry, S. M. & El-Kerdawy, M. M. (2011). *Eur. J. Med. Chem.* **46**, 3714–3720.
- Farrugia, L. J. (2012). *J. Appl. Cryst.* **45**, 849–854.
- Groom, C. R., Bruno, I. J., Lightfoot, M. P. & Ward, S. C. (2016). *Acta Cryst.* **B72**, 171–179.
- Gulcin, I. & Taslimi, P. (2018). *Expert Opin. Ther. Pat.* **28**, 541–549.
- Gunasekaran, B., Sureshbabu, R., Mohanakrishnan, A. K., Chakkaravarthi, G. & Manivannan, V. (2009). *Acta Cryst.* **E65**, o2069.
- Hanafy, A., Uno, J., Mitani, H., Kang, Y. & Mikami, Y. (2007). *Nippon Ishinkin Gakkai Zasshi*, **48**, 47–50.
- Krause, L., Herbst-Irmer, R., Sheldrick, G. M. & Stalke, D. (2015). *J. Appl. Cryst.* **48**, 3–10.
- Lima, C. F. R. A. C., Sousa, C. A. D., Rodriguez-Borges, J. E., Melo, A., Gomes, L. R., Low, J. N. & Santos, L. M. N. B. F. (2010). *Phys. Chem. Chem. Phys.* **12**, 11228–11237.
- Macrae, C. F., Sovago, I., Cottrell, S. J., Galek, P. T. A., McCabe, P., Pidcock, E., Platings, M., Shields, G. P., Stevens, J. S., Towler, M. & Wood, P. A. (2020). *J. Appl. Cryst.* **53**, 226–235.
- Madhan, S., NizamMohideen, M., Harikrishnan, K. & MohanaKrishnan, A. K. (2024a). *Acta Cryst.* **E80**, 682–690.
- Madhan, S., NizamMohideen, M., Pavunkumar, V. & MohanaKrishnan, A. K. (2022). *Acta Cryst.* **E78**, 1198–1203.
- Madhan, S., NizamMohideen, M., Pavunkumar, V. & MohanaKrishnan, A. K. (2023a). *Acta Cryst.* **E79**, 521–525.
- Madhan, S., NizamMohideen, M., Pavunkumar, V. & MohanaKrishnan, A. K. (2023b). *Acta Cryst.* **E79**, 741–746.
- Madhan, S., NizamMohideen, M., Pavunkumar, V. & MohanaKrishnan, A. K. (2024b). *Acta Cryst.* **E80**, 845–851.
- McKinnon, J. J., Jayatilaka, D. & Spackman, M. A. (2007). *Chem. Commun.* pp. 3814–3816.
- Murphy, C. D. (2003). *J. Appl. Microbiol.* **94**, 539–548.
- Ovung, A. & Bhattacharyya, J. (2021). *Biophys. Rev.* **13**, 259–272.
- Ramathilagam, C., Saravanan, V., Mohanakrishnan, A. K., Chakkaravarthi, G., Umarani, P. R. & Manivannan, V. (2011). *Acta Cryst.* **E67**, o632.
- Scozzafava, A., Owa, T., Mastrolorenzo, A. & Supuran, C. T. (2003). *Curr. Med. Chem.* **10**, 925–953.
- Sheldrick, G. M. (2015a). *Acta Cryst.* **A71**, 3–8.
- Sheldrick, G. M. (2015b). *Acta Cryst.* **C71**, 3–8.
- Spackman, M. A. & Jayatilaka, D. (2009). *CrystEngComm*, **11**, 19–32.
- Spackman, P. R., Turner, M. J., McKinnon, J. J., Wolff, S. K., Grimwood, D. J., Jayatilaka, D. & Spackman, M. A. (2021). *J. Appl. Cryst.* **54**, 1006–1011.
- Spek, A. L. (2020). *Acta Cryst.* **E76**, 1–11.
- Suparan, C. T., Briganti, F., Tilli, S., Chegwidden, W. R. & Scozzafava, A. (2001). *Bioorg. Med. Chem.* **9**, 703–714.
- Umadevi, M., Saravanan, V., Yamuna, R., Mohanakrishnan, A. K. & Chakkaravarthi, G. (2013). *Acta Cryst.* **E69**, o1802–o1803.
- Westrip, S. P. (2010). *J. Appl. Cryst.* **43**, 920–925.
- Zhao, Y., Shadrack, W. R., Wallace, M. J., Wu, Y., Griffith, E. C., Qi, J., Yun, M., White, S. W. & Lee, R. E. (2016). *Bioorg. Med. Chem. Lett.* **26**, 3950–3954.

supporting information

Acta Cryst. (2024). E80, 1110-1117 [https://doi.org/10.1107/S2056989024009587]

The crystal structures determination and Hirshfeld surface analysis of *N*-(4-bromo-3-methoxyphenyl)- and *N*-{[3-bromo-1-(phenylsulfonyl)-1*H*-indol-2-yl]methyl}- derivatives of *N*-{[3-bromo-1-(phenylsulfonyl)-1*H*-indol-2-yl]methyl}benzenesulfonamide

S. Madhan, M. NizamMohideen, Vinayagam Pavunkumar and Arasambattu K. MohanaKrishnan

Computing details

N-{[3-Bromo-1-(phenylsulfonyl)-1*H*-indol-2-yl]methyl}-*N*-(4-bromo-3-methoxyphenyl)benzenesulfonamide (I)

Crystal data

$C_{28}H_{22}Br_2N_2O_5S_2$

$M_r = 690.41$

Monoclinic, $P2_1/n$

$a = 9.5718$ (6) Å

$b = 14.4498$ (8) Å

$c = 20.0041$ (12) Å

$\beta = 92.874$ (2)°

$V = 2763.3$ (3) Å³

$Z = 4$

$F(000) = 1384$

$D_x = 1.660$ Mg m⁻³

Mo $K\alpha$ radiation, $\lambda = 0.71073$ Å

Cell parameters from 90697 reflections

$\theta = 1.4$ – 25.0 °

$\mu = 3.13$ mm⁻¹

$T = 303$ K

Block, colorless

$0.29 \times 0.24 \times 0.20$ mm

Data collection

Bruker D8 Venture Diffractometer

Radiation source: micro focus sealed tube

ω and φ scans

Absorption correction: multi-scan

(*SADABS*; Krause *et al.*, 2015)

$T_{\min} = 0.589$, $T_{\max} = 0.753$

90697 measured reflections

5234 independent reflections

4173 reflections with $I > 2\sigma(I)$

$R_{\text{int}} = 0.071$

$\theta_{\max} = 25.7$ °, $\theta_{\min} = 2.5$ °

$h = -11 \rightarrow 11$

$k = -17 \rightarrow 17$

$l = -24 \rightarrow 24$

Refinement

Refinement on F^2

Least-squares matrix: full

$R[F^2 > 2\sigma(F^2)] = 0.040$

$wR(F^2) = 0.099$

$S = 1.05$

5234 reflections

353 parameters

0 restraints

Hydrogen site location: inferred from neighbouring sites

H-atom parameters constrained

$w = 1/[\sigma^2(F_o^2) + (0.0293P)^2 + 5.9561P]$

where $P = (F_o^2 + 2F_c^2)/3$

$(\Delta/\sigma)_{\max} = 0.001$

$\Delta\rho_{\max} = 1.74$ e Å⁻³

$\Delta\rho_{\min} = -1.41$ e Å⁻³

Special details

Geometry. All esds (except the esd in the dihedral angle between two l.s. planes) are estimated using the full covariance matrix. The cell esds are taken into account individually in the estimation of esds in distances, angles and torsion angles; correlations between esds in cell parameters are only used when they are defined by crystal symmetry. An approximate (isotropic) treatment of cell esds is used for estimating esds involving l.s. planes.

Fractional atomic coordinates and isotropic or equivalent isotropic displacement parameters (\AA^2)

	<i>x</i>	<i>y</i>	<i>z</i>	$U_{\text{iso}}^*/U_{\text{eq}}$
C1	0.5912 (4)	0.6131 (2)	0.46145 (17)	0.0360 (8)
C2	0.7216 (4)	0.6188 (3)	0.4946 (2)	0.0485 (9)
H2	0.746482	0.669420	0.521272	0.058*
C3	0.8133 (5)	0.5462 (3)	0.4864 (2)	0.0581 (11)
H3	0.901819	0.548866	0.507653	0.070*
C4	0.7775 (5)	0.4695 (3)	0.4473 (2)	0.0575 (11)
H4	0.841931	0.421970	0.443087	0.069*
C5	0.6482 (5)	0.4633 (3)	0.41506 (19)	0.0486 (10)
H5	0.623774	0.411785	0.389142	0.058*
C6	0.5536 (4)	0.5362 (2)	0.42199 (17)	0.0372 (8)
C7	0.4158 (4)	0.5529 (2)	0.39470 (17)	0.0397 (8)
C8	0.3685 (4)	0.6356 (2)	0.41568 (16)	0.0337 (7)
C9	0.5386 (4)	0.8611 (2)	0.46312 (18)	0.0401 (8)
C10	0.6823 (5)	0.8709 (3)	0.4644 (3)	0.0610 (12)
H10	0.740032	0.827279	0.485932	0.073*
C11	0.7389 (6)	0.9465 (3)	0.4332 (3)	0.0775 (16)
H11	0.835512	0.953850	0.433711	0.093*
C12	0.6537 (6)	1.0105 (3)	0.4017 (2)	0.0686 (14)
H12	0.692625	1.061212	0.380876	0.082*
C13	0.5117 (6)	1.0007 (3)	0.4006 (2)	0.0617 (12)
H13	0.454818	1.044675	0.379011	0.074*
C14	0.4518 (5)	0.9258 (3)	0.43145 (19)	0.0479 (9)
H14	0.355072	0.919091	0.430866	0.057*
C15	0.2288 (4)	0.6783 (3)	0.39902 (17)	0.0374 (8)
H15A	0.168446	0.632698	0.376678	0.045*
H15B	0.186408	0.696104	0.440144	0.045*
C16	-0.0367 (4)	0.7764 (3)	0.31156 (18)	0.0404 (8)
C17	-0.1273 (4)	0.7228 (3)	0.3466 (2)	0.0544 (11)
H17	-0.117432	0.718441	0.392956	0.065*
C18	-0.2334 (5)	0.6754 (3)	0.3113 (2)	0.0640 (12)
H18	-0.296109	0.639804	0.334362	0.077*
C19	-0.2469 (4)	0.6806 (3)	0.2427 (2)	0.0564 (11)
H19	-0.317930	0.648112	0.219529	0.068*
C20	-0.1556 (4)	0.7338 (3)	0.2082 (2)	0.0557 (11)
H20	-0.165121	0.737115	0.161734	0.067*
C21	-0.0501 (4)	0.7820 (3)	0.2420 (2)	0.0508 (10)
H21	0.011626	0.818004	0.218646	0.061*
C22	0.2982 (4)	0.7476 (2)	0.29018 (16)	0.0347 (8)
C23	0.2612 (4)	0.6733 (3)	0.24960 (19)	0.0453 (9)

H23	0.195602	0.630544	0.263040	0.054*
C24	0.3227 (4)	0.6627 (3)	0.18851 (18)	0.0482 (10)
H24	0.300825	0.611588	0.161749	0.058*
C25	0.4159 (4)	0.7279 (3)	0.16766 (17)	0.0395 (8)
C26	0.4523 (4)	0.8037 (3)	0.20774 (18)	0.0405 (8)
C27	0.3937 (4)	0.8122 (3)	0.26980 (18)	0.0386 (8)
H27	0.418840	0.861639	0.297649	0.046*
C28	0.5954 (7)	0.9366 (4)	0.2262 (3)	0.090 (2)
H28A	0.519832	0.977821	0.235067	0.135*
H28B	0.667708	0.970260	0.205184	0.135*
H28C	0.632434	0.910622	0.267595	0.135*
N1	0.4763 (3)	0.67482 (19)	0.45867 (14)	0.0344 (6)
N2	0.2386 (3)	0.7612 (2)	0.35510 (14)	0.0356 (6)
O1	0.5542 (3)	0.75110 (19)	0.56538 (13)	0.0516 (7)
O2	0.3206 (3)	0.78625 (18)	0.51436 (13)	0.0488 (7)
O3	0.1411 (3)	0.91308 (19)	0.31900 (14)	0.0516 (7)
O4	0.0678 (3)	0.8422 (2)	0.42399 (13)	0.0552 (7)
O5	0.5454 (3)	0.8642 (2)	0.18304 (14)	0.0589 (8)
S1	0.46528 (10)	0.76919 (6)	0.50760 (4)	0.0375 (2)
S2	0.10295 (10)	0.83326 (7)	0.35581 (5)	0.0412 (2)
Br1	0.50238 (5)	0.71099 (4)	0.08522 (2)	0.05801 (14)
Br2	0.31588 (6)	0.46768 (3)	0.34009 (2)	0.06813 (17)

Atomic displacement parameters (Å²)

	U^{11}	U^{22}	U^{33}	U^{12}	U^{13}	U^{23}
C1	0.0391 (19)	0.0333 (18)	0.0364 (18)	0.0038 (15)	0.0097 (15)	0.0063 (15)
C2	0.043 (2)	0.044 (2)	0.059 (2)	0.0010 (17)	0.0015 (18)	0.0019 (19)
C3	0.044 (2)	0.062 (3)	0.068 (3)	0.013 (2)	0.003 (2)	0.009 (2)
C4	0.060 (3)	0.052 (3)	0.061 (3)	0.024 (2)	0.014 (2)	0.009 (2)
C5	0.067 (3)	0.038 (2)	0.042 (2)	0.0142 (19)	0.0155 (19)	0.0004 (17)
C6	0.048 (2)	0.0349 (18)	0.0295 (17)	0.0050 (16)	0.0095 (15)	0.0036 (14)
C7	0.054 (2)	0.0360 (19)	0.0289 (17)	0.0034 (17)	0.0023 (16)	-0.0022 (15)
C8	0.042 (2)	0.0340 (18)	0.0251 (16)	-0.0003 (15)	0.0038 (14)	0.0010 (14)
C9	0.050 (2)	0.0294 (18)	0.042 (2)	0.0005 (16)	0.0067 (16)	-0.0062 (15)
C10	0.049 (3)	0.038 (2)	0.097 (4)	0.0055 (19)	0.016 (2)	0.003 (2)
C11	0.066 (3)	0.054 (3)	0.117 (5)	-0.004 (2)	0.041 (3)	-0.002 (3)
C12	0.102 (4)	0.038 (2)	0.068 (3)	-0.008 (3)	0.032 (3)	-0.001 (2)
C13	0.096 (4)	0.038 (2)	0.051 (3)	0.004 (2)	-0.003 (2)	-0.0018 (19)
C14	0.058 (2)	0.039 (2)	0.045 (2)	0.0029 (18)	-0.0065 (18)	-0.0071 (17)
C15	0.0388 (19)	0.042 (2)	0.0314 (17)	-0.0015 (16)	0.0040 (14)	0.0008 (15)
C16	0.0337 (19)	0.045 (2)	0.043 (2)	0.0061 (16)	0.0080 (15)	0.0088 (16)
C17	0.051 (2)	0.070 (3)	0.044 (2)	-0.001 (2)	0.0175 (19)	0.011 (2)
C18	0.054 (3)	0.071 (3)	0.069 (3)	-0.010 (2)	0.025 (2)	0.011 (2)
C19	0.041 (2)	0.059 (3)	0.069 (3)	0.000 (2)	0.000 (2)	0.004 (2)
C20	0.053 (3)	0.071 (3)	0.043 (2)	-0.002 (2)	-0.0014 (19)	0.011 (2)
C21	0.046 (2)	0.063 (3)	0.044 (2)	-0.006 (2)	0.0044 (18)	0.0190 (19)
C22	0.0319 (18)	0.043 (2)	0.0296 (17)	0.0069 (15)	0.0018 (14)	0.0011 (15)

C23	0.044 (2)	0.053 (2)	0.0390 (19)	-0.0077 (18)	0.0043 (16)	-0.0029 (17)
C24	0.050 (2)	0.061 (3)	0.0338 (19)	-0.004 (2)	-0.0002 (17)	-0.0115 (18)
C25	0.0339 (19)	0.057 (2)	0.0271 (16)	0.0076 (17)	0.0033 (14)	-0.0004 (16)
C26	0.0366 (19)	0.045 (2)	0.0407 (19)	0.0022 (16)	0.0082 (15)	0.0017 (17)
C27	0.0382 (19)	0.0396 (19)	0.0384 (19)	0.0015 (16)	0.0060 (15)	-0.0028 (15)
C28	0.109 (4)	0.078 (4)	0.086 (4)	-0.049 (3)	0.052 (3)	-0.028 (3)
N1	0.0377 (16)	0.0299 (14)	0.0358 (15)	0.0025 (12)	0.0041 (12)	-0.0035 (12)
N2	0.0369 (16)	0.0411 (16)	0.0291 (14)	0.0056 (13)	0.0047 (12)	0.0027 (12)
O1	0.0678 (19)	0.0501 (16)	0.0359 (14)	0.0026 (14)	-0.0065 (13)	-0.0033 (12)
O2	0.0461 (15)	0.0508 (16)	0.0508 (16)	0.0035 (13)	0.0147 (12)	-0.0137 (13)
O3	0.0532 (17)	0.0416 (15)	0.0599 (17)	0.0042 (13)	0.0024 (13)	0.0061 (13)
O4	0.0559 (17)	0.0688 (19)	0.0412 (15)	0.0214 (15)	0.0073 (13)	-0.0074 (14)
O5	0.068 (2)	0.0602 (18)	0.0507 (17)	-0.0152 (15)	0.0275 (15)	-0.0064 (14)
S1	0.0441 (5)	0.0353 (4)	0.0334 (4)	0.0024 (4)	0.0055 (4)	-0.0053 (4)
S2	0.0402 (5)	0.0451 (5)	0.0384 (5)	0.0088 (4)	0.0055 (4)	0.0014 (4)
Br1	0.0547 (3)	0.0844 (3)	0.0358 (2)	0.0026 (2)	0.01070 (17)	-0.0083 (2)
Br2	0.0946 (4)	0.0496 (3)	0.0575 (3)	0.0103 (2)	-0.0228 (2)	-0.0210 (2)

Geometric parameters (Å, °)

C1—C2	1.386 (5)	C16—S2	1.768 (4)
C1—C6	1.399 (5)	C17—C18	1.388 (6)
C1—N1	1.415 (4)	C17—H17	0.9300
C2—C3	1.382 (6)	C18—C19	1.375 (6)
C2—H2	0.9300	C18—H18	0.9300
C3—C4	1.388 (6)	C19—C20	1.375 (6)
C3—H3	0.9300	C19—H19	0.9300
C4—C5	1.370 (6)	C20—C21	1.377 (6)
C4—H4	0.9300	C20—H20	0.9300
C5—C6	1.400 (5)	C21—H21	0.9300
C5—H5	0.9300	C22—C23	1.381 (5)
C6—C7	1.423 (5)	C22—C27	1.383 (5)
C7—C8	1.352 (5)	C22—N2	1.457 (4)
C7—Br2	1.876 (4)	C23—C24	1.391 (5)
C8—N1	1.427 (4)	C23—H23	0.9300
C8—C15	1.495 (5)	C24—C25	1.377 (5)
C9—C10	1.381 (6)	C24—H24	0.9300
C9—C14	1.384 (5)	C25—C26	1.391 (5)
C9—S1	1.764 (4)	C25—Br1	1.898 (3)
C10—C11	1.382 (6)	C26—O5	1.358 (4)
C10—H10	0.9300	C26—C27	1.394 (5)
C11—C12	1.367 (7)	C27—H27	0.9300
C11—H11	0.9300	C28—O5	1.425 (6)
C12—C13	1.365 (7)	C28—H28A	0.9600
C12—H12	0.9300	C28—H28B	0.9600
C13—C14	1.384 (6)	C28—H28C	0.9600
C13—H13	0.9300	N1—S1	1.685 (3)
C14—H14	0.9300	N2—S2	1.665 (3)

C15—N2	1.491 (4)	O1—S1	1.425 (3)
C15—H15A	0.9700	O2—S1	1.420 (3)
C15—H15B	0.9700	O3—S2	1.426 (3)
C16—C17	1.380 (5)	O4—S2	1.427 (3)
C16—C21	1.393 (5)		
C2—C1—C6	121.1 (3)	C19—C18—H18	119.7
C2—C1—N1	131.4 (3)	C17—C18—H18	119.7
C6—C1—N1	107.5 (3)	C18—C19—C20	120.1 (4)
C3—C2—C1	117.4 (4)	C18—C19—H19	120.0
C3—C2—H2	121.3	C20—C19—H19	120.0
C1—C2—H2	121.3	C19—C20—C21	120.4 (4)
C2—C3—C4	122.2 (4)	C19—C20—H20	119.8
C2—C3—H3	118.9	C21—C20—H20	119.8
C4—C3—H3	118.9	C20—C21—C16	119.3 (4)
C5—C4—C3	120.6 (4)	C20—C21—H21	120.3
C5—C4—H4	119.7	C16—C21—H21	120.3
C3—C4—H4	119.7	C23—C22—C27	120.4 (3)
C4—C5—C6	118.5 (4)	C23—C22—N2	121.9 (3)
C4—C5—H5	120.8	C27—C22—N2	117.7 (3)
C6—C5—H5	120.8	C22—C23—C24	119.6 (4)
C1—C6—C5	120.3 (4)	C22—C23—H23	120.2
C1—C6—C7	106.8 (3)	C24—C23—H23	120.2
C5—C6—C7	132.9 (4)	C25—C24—C23	120.0 (4)
C8—C7—C6	110.5 (3)	C25—C24—H24	120.0
C8—C7—Br2	126.3 (3)	C23—C24—H24	120.0
C6—C7—Br2	123.2 (3)	C24—C25—C26	120.8 (3)
C7—C8—N1	107.1 (3)	C24—C25—Br1	119.5 (3)
C7—C8—C15	127.2 (3)	C26—C25—Br1	119.6 (3)
N1—C8—C15	125.6 (3)	O5—C26—C25	116.5 (3)
C10—C9—C14	120.9 (4)	O5—C26—C27	124.6 (3)
C10—C9—S1	119.3 (3)	C25—C26—C27	118.8 (3)
C14—C9—S1	119.6 (3)	C22—C27—C26	120.3 (3)
C9—C10—C11	119.1 (4)	C22—C27—H27	119.8
C9—C10—H10	120.5	C26—C27—H27	119.8
C11—C10—H10	120.5	O5—C28—H28A	109.5
C12—C11—C10	120.3 (5)	O5—C28—H28B	109.5
C12—C11—H11	119.9	H28A—C28—H28B	109.5
C10—C11—H11	119.9	O5—C28—H28C	109.5
C13—C12—C11	120.5 (4)	H28A—C28—H28C	109.5
C13—C12—H12	119.8	H28B—C28—H28C	109.5
C11—C12—H12	119.8	C1—N1—C8	108.1 (3)
C12—C13—C14	120.6 (4)	C1—N1—S1	124.0 (2)
C12—C13—H13	119.7	C8—N1—S1	127.4 (2)
C14—C13—H13	119.7	C22—N2—C15	117.1 (3)
C9—C14—C13	118.6 (4)	C22—N2—S2	115.6 (2)
C9—C14—H14	120.7	C15—N2—S2	115.1 (2)
C13—C14—H14	120.7	C26—O5—C28	117.3 (3)

N2—C15—C8	112.3 (3)	O2—S1—O1	120.03 (17)
N2—C15—H15A	109.1	O2—S1—N1	106.60 (15)
C8—C15—H15A	109.1	O1—S1—N1	105.69 (15)
N2—C15—H15B	109.1	O2—S1—C9	109.41 (18)
C8—C15—H15B	109.1	O1—S1—C9	108.10 (18)
H15A—C15—H15B	107.9	N1—S1—C9	106.14 (15)
C17—C16—C21	120.7 (4)	O3—S2—O4	119.92 (18)
C17—C16—S2	119.0 (3)	O3—S2—N2	106.35 (16)
C21—C16—S2	120.1 (3)	O4—S2—N2	106.66 (15)
C16—C17—C18	118.8 (4)	O3—S2—C16	108.91 (17)
C16—C17—H17	120.6	O4—S2—C16	108.18 (18)
C18—C17—H17	120.6	N2—S2—C16	105.98 (16)
C19—C18—C17	120.7 (4)		
C6—C1—C2—C3	0.8 (6)	Br1—C25—C26—C27	-176.4 (3)
N1—C1—C2—C3	-179.1 (4)	C23—C22—C27—C26	0.8 (5)
C1—C2—C3—C4	-0.8 (6)	N2—C22—C27—C26	-178.9 (3)
C2—C3—C4—C5	0.2 (7)	O5—C26—C27—C22	179.1 (3)
C3—C4—C5—C6	0.4 (6)	C25—C26—C27—C22	-1.7 (5)
C2—C1—C6—C5	-0.2 (5)	C2—C1—N1—C8	178.6 (4)
N1—C1—C6—C5	179.7 (3)	C6—C1—N1—C8	-1.2 (4)
C2—C1—C6—C7	-179.1 (3)	C2—C1—N1—S1	-9.6 (5)
N1—C1—C6—C7	0.8 (4)	C6—C1—N1—S1	170.5 (2)
C4—C5—C6—C1	-0.4 (5)	C7—C8—N1—C1	1.2 (4)
C4—C5—C6—C7	178.1 (4)	C15—C8—N1—C1	179.8 (3)
C1—C6—C7—C8	-0.1 (4)	C7—C8—N1—S1	-170.2 (3)
C5—C6—C7—C8	-178.7 (4)	C15—C8—N1—S1	8.4 (5)
C1—C6—C7—Br2	-177.9 (2)	C23—C22—N2—C15	44.3 (5)
C5—C6—C7—Br2	3.4 (6)	C27—C22—N2—C15	-136.0 (3)
C6—C7—C8—N1	-0.7 (4)	C23—C22—N2—S2	-96.5 (4)
Br2—C7—C8—N1	177.1 (2)	C27—C22—N2—S2	83.3 (3)
C6—C7—C8—C15	-179.3 (3)	C8—C15—N2—C22	59.7 (4)
Br2—C7—C8—C15	-1.5 (5)	C8—C15—N2—S2	-159.4 (2)
C14—C9—C10—C11	-0.3 (7)	C25—C26—O5—C28	-173.4 (4)
S1—C9—C10—C11	-175.7 (4)	C27—C26—O5—C28	5.8 (6)
C9—C10—C11—C12	0.1 (8)	C1—N1—S1—O2	-152.6 (3)
C10—C11—C12—C13	0.0 (8)	C8—N1—S1—O2	17.5 (3)
C11—C12—C13—C14	0.1 (7)	C1—N1—S1—O1	-23.9 (3)
C10—C9—C14—C13	0.3 (6)	C8—N1—S1—O1	146.3 (3)
S1—C9—C14—C13	175.7 (3)	C1—N1—S1—C9	90.8 (3)
C12—C13—C14—C9	-0.2 (6)	C8—N1—S1—C9	-99.1 (3)
C7—C8—C15—N2	-111.1 (4)	C10—C9—S1—O2	164.5 (3)
N1—C8—C15—N2	70.5 (4)	C14—C9—S1—O2	-11.0 (3)
C21—C16—C17—C18	-0.9 (6)	C10—C9—S1—O1	32.2 (4)
S2—C16—C17—C18	-177.5 (3)	C14—C9—S1—O1	-143.3 (3)
C16—C17—C18—C19	1.0 (7)	C10—C9—S1—N1	-80.8 (4)
C17—C18—C19—C20	-0.6 (7)	C14—C9—S1—N1	103.7 (3)
C18—C19—C20—C21	0.1 (7)	C22—N2—S2—O3	-46.6 (3)

C19—C20—C21—C16	0.1 (7)	C15—N2—S2—O3	171.8 (2)
C17—C16—C21—C20	0.4 (6)	C22—N2—S2—O4	-175.7 (3)
S2—C16—C21—C20	177.0 (3)	C15—N2—S2—O4	42.8 (3)
C27—C22—C23—C24	1.3 (6)	C22—N2—S2—C16	69.2 (3)
N2—C22—C23—C24	-179.0 (3)	C15—N2—S2—C16	-72.3 (3)
C22—C23—C24—C25	-2.4 (6)	C17—C16—S2—O3	-153.9 (3)
C23—C24—C25—C26	1.5 (6)	C21—C16—S2—O3	29.4 (4)
C23—C24—C25—Br1	178.5 (3)	C17—C16—S2—O4	-22.0 (4)
C24—C25—C26—O5	179.8 (4)	C21—C16—S2—O4	161.3 (3)
Br1—C25—C26—O5	2.8 (5)	C17—C16—S2—N2	92.0 (3)
C24—C25—C26—C27	0.5 (6)	C21—C16—S2—N2	-84.6 (3)

Hydrogen-bond geometry (Å, °)

<i>D</i> —H... <i>A</i>	<i>D</i> —H	H... <i>A</i>	<i>D</i> ... <i>A</i>	<i>D</i> —H... <i>A</i>
C2—H2...O1	0.93	2.39	2.908 (5)	115
C11—H11...O4 ⁱ	0.93	2.76	3.503 (6)	137
C15—H15B...O2	0.97	2.31	2.886 (4)	117
C18—H18...Cg(N1/C1/C6—C8) ⁱⁱ	0.93	2.99	3.861 (8)	156
C18—H18...Cg(C1—C6) ⁱⁱ	0.93	2.81	3.579 (1)	141

Symmetry codes: (i) $x+1, y, z$; (ii) $x-1, y, z$.*N,N*-Bis[3-bromo-1-(phenylsulfonyl)-1*H*-indol-2-yl]methyl]benzenesulfonamide (II)

Crystal data

 $C_{36}H_{27}Br_2N_3O_6S_3$ $M_r = 853.60$ Monoclinic, $P2_1/n$ $a = 8.2664$ (4) Å $b = 34.7886$ (18) Å $c = 12.5972$ (6) Å $\beta = 104.550$ (2)° $V = 3506.5$ (3) Å³ $Z = 4$ $F(000) = 1720$ $D_x = 1.617$ Mg m⁻³Mo $K\alpha$ radiation, $\lambda = 0.71073$ Å

Cell parameters from 73921 reflections

 $\theta = 1.4$ – 25.0 ° $\mu = 2.54$ mm⁻¹ $T = 303$ K

Block, colorless

 $0.29 \times 0.19 \times 0.04$ mm

Data collection

Bruker D8 Venture Diffractometer

Radiation source: micro focus sealed tube

 ω and ϕ scans

Absorption correction: multi-scan

(SADABS; Krause *et al.*, 2015) $T_{\min} = 0.491$, $T_{\max} = 0.745$

73921 measured reflections

6434 independent reflections

5196 reflections with $I > 2\sigma(I)$ $R_{\text{int}} = 0.071$ $\theta_{\text{max}} = 25.5$ °, $\theta_{\text{min}} = 2.7$ ° $h = -9 \rightarrow 9$ $k = -41 \rightarrow 41$ $l = -15 \rightarrow 15$

Refinement

Refinement on F^2

Least-squares matrix: full

 $R[F^2 > 2\sigma(F^2)] = 0.048$ $wR(F^2) = 0.120$ $S = 1.12$

6434 reflections

451 parameters

0 restraints

Hydrogen site location: inferred from neighbouring sites

H-atom parameters constrained

$$w = 1/[\sigma^2(F_o^2) + (0.0397P)^2 + 5.0983P]$$

where $P = (F_o^2 + 2F_c^2)/3$
 $(\Delta/\sigma)_{\max} = 0.001$

$$\Delta\rho_{\max} = 0.46 \text{ e } \text{\AA}^{-3}$$

$$\Delta\rho_{\min} = -0.47 \text{ e } \text{\AA}^{-3}$$

Special details

Geometry. All esds (except the esd in the dihedral angle between two l.s. planes) are estimated using the full covariance matrix. The cell esds are taken into account individually in the estimation of esds in distances, angles and torsion angles; correlations between esds in cell parameters are only used when they are defined by crystal symmetry. An approximate (isotropic) treatment of cell esds is used for estimating esds involving l.s. planes.

Fractional atomic coordinates and isotropic or equivalent isotropic displacement parameters (\AA^2)

	<i>x</i>	<i>y</i>	<i>z</i>	$U_{\text{iso}}^*/U_{\text{eq}}$
C1	0.2266 (5)	0.42112 (11)	0.6112 (3)	0.0474 (10)
C2	0.2075 (6)	0.45836 (12)	0.5688 (4)	0.0691 (14)
H2	0.242319	0.465117	0.506636	0.083*
C3	0.1341 (8)	0.48456 (15)	0.6241 (6)	0.090 (2)
H3	0.119704	0.509708	0.598397	0.108*
C4	0.0814 (7)	0.47499 (17)	0.7155 (6)	0.091 (2)
H4	0.032049	0.493682	0.749854	0.109*
C5	0.1002 (5)	0.43816 (16)	0.7576 (4)	0.0700 (14)
H5	0.065741	0.431822	0.820239	0.084*
C6	0.1726 (5)	0.41075 (12)	0.7029 (3)	0.0482 (10)
C7	0.2180 (5)	0.37117 (11)	0.7239 (3)	0.0432 (9)
C8	0.2986 (4)	0.35808 (10)	0.6506 (3)	0.0361 (8)
C9	0.0542 (5)	0.37495 (11)	0.3929 (3)	0.0431 (9)
C10	-0.0441 (6)	0.40600 (13)	0.3488 (3)	0.0568 (11)
H10	0.004062	0.429860	0.343575	0.068*
C11	-0.2147 (7)	0.40109 (18)	0.3127 (4)	0.0713 (14)
H11	-0.282247	0.421807	0.283294	0.086*
C12	-0.2844 (6)	0.36617 (19)	0.3199 (4)	0.0747 (15)
H12	-0.399556	0.363131	0.295081	0.090*
C13	-0.1865 (6)	0.33531 (16)	0.3634 (4)	0.0711 (14)
H13	-0.235668	0.311493	0.367608	0.085*
C14	-0.0158 (6)	0.33944 (12)	0.4008 (4)	0.0564 (11)
H14	0.050914	0.318655	0.430778	0.068*
C15	0.3938 (5)	0.32126 (10)	0.6489 (3)	0.0416 (9)
H15A	0.315178	0.300654	0.621888	0.050*
H15B	0.464582	0.324063	0.598503	0.050*
C16	0.6415 (5)	0.24696 (10)	0.6959 (3)	0.0429 (9)
C17	0.8099 (6)	0.24045 (14)	0.7415 (4)	0.0619 (12)
H17	0.853833	0.242415	0.816857	0.074*
C18	0.9117 (7)	0.23100 (17)	0.6738 (6)	0.0870 (18)
H18	1.024933	0.226412	0.703439	0.104*
C19	0.8454 (10)	0.22842 (16)	0.5629 (6)	0.091 (2)
H19	0.914182	0.222430	0.517049	0.109*
C20	0.6786 (10)	0.23460 (17)	0.5192 (4)	0.094 (2)
H20	0.634731	0.232593	0.443842	0.113*
C21	0.5756 (7)	0.24368 (13)	0.5848 (4)	0.0671 (14)

H21	0.462055	0.247598	0.554608	0.081*
C22	0.6628 (5)	0.33072 (11)	0.7938 (3)	0.0455 (9)
H22A	0.717555	0.322827	0.868007	0.055*
H22B	0.732885	0.322749	0.746573	0.055*
C23	0.6489 (4)	0.37330 (11)	0.7907 (3)	0.0390 (8)
C24	0.6816 (5)	0.39717 (12)	0.7143 (3)	0.0454 (9)
C25	0.6421 (5)	0.43593 (12)	0.7368 (3)	0.0462 (9)
C26	0.6451 (6)	0.47079 (14)	0.6812 (4)	0.0646 (13)
H26	0.682286	0.471908	0.617395	0.078*
C27	0.5912 (7)	0.50320 (14)	0.7244 (5)	0.0746 (15)
H27	0.592151	0.526653	0.689090	0.090*
C28	0.5358 (7)	0.50180 (13)	0.8183 (5)	0.0706 (14)
H28	0.501929	0.524470	0.845424	0.085*
C29	0.5286 (5)	0.46829 (12)	0.8734 (4)	0.0541 (11)
H29	0.487987	0.467571	0.935870	0.065*
C30	0.5854 (5)	0.43506 (10)	0.8315 (3)	0.0415 (9)
C31	0.8482 (5)	0.39173 (12)	1.0480 (3)	0.0443 (9)
C32	0.9122 (6)	0.42849 (16)	1.0514 (4)	0.0699 (14)
H32	0.841943	0.449515	1.030325	0.084*
C33	1.0838 (8)	0.4333 (2)	1.0869 (5)	0.094 (2)
H33	1.130676	0.457639	1.088526	0.113*
C34	1.1843 (7)	0.4018 (3)	1.1197 (5)	0.098 (2)
H34	1.299428	0.405079	1.142745	0.117*
C35	1.1190 (7)	0.3657 (2)	1.1194 (5)	0.0891 (19)
H35	1.188587	0.344814	1.144262	0.107*
C36	0.9479 (6)	0.36050 (15)	1.0816 (4)	0.0664 (13)
H36	0.901555	0.336052	1.079059	0.080*
N1	0.3054 (4)	0.38863 (8)	0.5760 (2)	0.0400 (7)
N2	0.4990 (4)	0.31064 (8)	0.7588 (2)	0.0389 (7)
N3	0.5879 (4)	0.39605 (8)	0.8669 (2)	0.0375 (7)
O1	0.3214 (4)	0.41488 (10)	0.3958 (3)	0.0727 (9)
O2	0.3521 (4)	0.34514 (9)	0.4273 (2)	0.0566 (7)
O3	0.3523 (4)	0.24801 (9)	0.7430 (3)	0.0728 (10)
O4	0.6071 (5)	0.25830 (9)	0.8922 (2)	0.0659 (9)
O5	0.5475 (4)	0.41314 (9)	1.0495 (2)	0.0549 (7)
O6	0.5948 (4)	0.34548 (8)	1.0092 (2)	0.0606 (8)
S1	0.27243 (13)	0.38060 (3)	0.43993 (8)	0.0467 (2)
S2	0.51553 (13)	0.26365 (3)	0.78055 (9)	0.0470 (2)
S3	0.63083 (12)	0.38513 (3)	1.00122 (8)	0.0416 (2)
Br1	0.74777 (6)	0.38250 (2)	0.58953 (4)	0.07276 (18)
Br2	0.17344 (7)	0.34427 (2)	0.84137 (4)	0.07746 (19)

Atomic displacement parameters (\AA^2)

	U^{11}	U^{22}	U^{33}	U^{12}	U^{13}	U^{23}
C1	0.042 (2)	0.038 (2)	0.052 (2)	0.0029 (17)	-0.0057 (18)	-0.0091 (18)
C2	0.078 (3)	0.040 (2)	0.071 (3)	0.008 (2)	-0.016 (3)	0.001 (2)
C3	0.091 (4)	0.044 (3)	0.110 (5)	0.023 (3)	-0.022 (4)	-0.021 (3)

C4	0.060 (3)	0.073 (4)	0.119 (5)	0.031 (3)	-0.019 (3)	-0.050 (4)
C5	0.045 (3)	0.083 (4)	0.076 (3)	0.017 (2)	0.004 (2)	-0.031 (3)
C6	0.0325 (19)	0.055 (2)	0.052 (2)	0.0094 (17)	0.0005 (17)	-0.0170 (19)
C7	0.036 (2)	0.054 (2)	0.038 (2)	0.0044 (17)	0.0058 (16)	-0.0004 (17)
C8	0.0357 (19)	0.0359 (19)	0.0353 (19)	0.0020 (15)	0.0061 (15)	0.0013 (15)
C9	0.051 (2)	0.046 (2)	0.0330 (19)	0.0019 (18)	0.0108 (17)	-0.0048 (16)
C10	0.067 (3)	0.058 (3)	0.040 (2)	0.007 (2)	0.004 (2)	0.0027 (19)
C11	0.071 (3)	0.091 (4)	0.044 (3)	0.025 (3)	0.000 (2)	-0.005 (2)
C12	0.052 (3)	0.111 (5)	0.058 (3)	0.001 (3)	0.007 (2)	-0.027 (3)
C13	0.065 (3)	0.080 (4)	0.068 (3)	-0.024 (3)	0.018 (3)	-0.024 (3)
C14	0.066 (3)	0.048 (2)	0.052 (3)	-0.004 (2)	0.008 (2)	-0.0083 (19)
C15	0.046 (2)	0.0311 (19)	0.046 (2)	0.0052 (16)	0.0086 (17)	-0.0013 (16)
C16	0.053 (2)	0.0288 (19)	0.045 (2)	0.0068 (16)	0.0103 (18)	0.0000 (16)
C17	0.051 (3)	0.071 (3)	0.061 (3)	0.007 (2)	0.009 (2)	-0.014 (2)
C18	0.057 (3)	0.092 (4)	0.116 (5)	0.008 (3)	0.030 (3)	-0.021 (4)
C19	0.134 (6)	0.070 (4)	0.093 (5)	0.018 (4)	0.075 (4)	0.003 (3)
C20	0.152 (6)	0.083 (4)	0.049 (3)	0.058 (4)	0.029 (3)	-0.002 (3)
C21	0.089 (4)	0.051 (3)	0.054 (3)	0.025 (2)	0.006 (3)	-0.010 (2)
C22	0.039 (2)	0.046 (2)	0.050 (2)	0.0004 (17)	0.0076 (17)	-0.0103 (18)
C23	0.0342 (19)	0.044 (2)	0.0376 (19)	-0.0023 (15)	0.0062 (15)	-0.0092 (16)
C24	0.038 (2)	0.059 (3)	0.041 (2)	-0.0138 (18)	0.0134 (17)	-0.0082 (18)
C25	0.042 (2)	0.049 (2)	0.045 (2)	-0.0151 (18)	0.0055 (18)	-0.0016 (18)
C26	0.061 (3)	0.068 (3)	0.063 (3)	-0.021 (2)	0.012 (2)	0.015 (2)
C27	0.077 (3)	0.047 (3)	0.087 (4)	-0.014 (2)	-0.003 (3)	0.019 (3)
C28	0.077 (3)	0.039 (3)	0.089 (4)	-0.001 (2)	0.009 (3)	0.000 (2)
C29	0.055 (3)	0.045 (2)	0.057 (3)	0.0029 (19)	0.004 (2)	-0.007 (2)
C30	0.042 (2)	0.035 (2)	0.043 (2)	-0.0041 (16)	0.0021 (17)	-0.0016 (16)
C31	0.043 (2)	0.059 (3)	0.0315 (19)	-0.0041 (18)	0.0097 (16)	-0.0073 (17)
C32	0.058 (3)	0.083 (4)	0.060 (3)	-0.018 (3)	0.000 (2)	0.007 (3)
C33	0.072 (4)	0.132 (6)	0.070 (4)	-0.053 (4)	0.004 (3)	0.007 (4)
C34	0.042 (3)	0.196 (8)	0.058 (3)	-0.008 (4)	0.019 (3)	-0.018 (4)
C35	0.053 (3)	0.134 (6)	0.073 (4)	0.028 (4)	0.002 (3)	-0.033 (4)
C36	0.060 (3)	0.074 (3)	0.061 (3)	0.013 (2)	0.007 (2)	-0.020 (2)
N1	0.0451 (17)	0.0349 (16)	0.0385 (17)	0.0024 (13)	0.0079 (14)	-0.0004 (13)
N2	0.0416 (17)	0.0309 (16)	0.0441 (17)	0.0046 (13)	0.0106 (14)	0.0029 (13)
N3	0.0416 (17)	0.0360 (16)	0.0348 (16)	-0.0013 (13)	0.0095 (13)	-0.0033 (12)
O1	0.083 (2)	0.072 (2)	0.063 (2)	-0.0196 (18)	0.0183 (18)	0.0201 (17)
O2	0.0584 (18)	0.068 (2)	0.0465 (16)	0.0097 (15)	0.0196 (14)	-0.0085 (14)
O3	0.0582 (19)	0.0482 (18)	0.118 (3)	-0.0067 (15)	0.034 (2)	0.0129 (18)
O4	0.099 (3)	0.0575 (19)	0.0452 (17)	0.0221 (17)	0.0260 (17)	0.0143 (14)
O5	0.0543 (17)	0.0699 (19)	0.0461 (16)	0.0056 (14)	0.0228 (14)	-0.0075 (14)
O6	0.074 (2)	0.0516 (18)	0.0562 (18)	-0.0182 (15)	0.0162 (16)	0.0063 (14)
S1	0.0528 (6)	0.0515 (6)	0.0365 (5)	-0.0042 (5)	0.0126 (4)	0.0050 (4)
S2	0.0541 (6)	0.0357 (5)	0.0551 (6)	0.0062 (4)	0.0211 (5)	0.0076 (4)
S3	0.0416 (5)	0.0473 (5)	0.0378 (5)	-0.0050 (4)	0.0136 (4)	-0.0027 (4)
Br1	0.0661 (3)	0.1085 (4)	0.0535 (3)	-0.0273 (3)	0.0333 (2)	-0.0247 (3)
Br2	0.0688 (3)	0.1127 (5)	0.0610 (3)	0.0127 (3)	0.0352 (3)	0.0225 (3)

Geometric parameters (Å, °)

C1—C6	1.387 (6)	C21—H21	0.9300
C1—C2	1.395 (6)	C22—C23	1.485 (5)
C1—N1	1.429 (5)	C22—N2	1.489 (5)
C2—C3	1.377 (8)	C22—H22A	0.9700
C2—H2	0.9300	C22—H22B	0.9700
C3—C4	1.371 (9)	C23—C24	1.348 (5)
C3—H3	0.9300	C23—N3	1.430 (4)
C4—C5	1.380 (8)	C24—C25	1.432 (6)
C4—H4	0.9300	C24—Br1	1.861 (4)
C5—C6	1.397 (6)	C25—C30	1.387 (6)
C5—H5	0.9300	C25—C26	1.405 (6)
C6—C7	1.434 (6)	C26—C27	1.374 (7)
C7—C8	1.347 (5)	C26—H26	0.9300
C7—Br2	1.864 (4)	C27—C28	1.373 (8)
C8—N1	1.429 (5)	C27—H27	0.9300
C8—C15	1.507 (5)	C28—C29	1.366 (6)
C9—C14	1.378 (6)	C28—H28	0.9300
C9—C10	1.381 (6)	C29—C30	1.400 (6)
C9—S1	1.763 (4)	C29—H29	0.9300
C10—C11	1.379 (7)	C30—N3	1.427 (5)
C10—H10	0.9300	C31—C36	1.365 (6)
C11—C12	1.357 (8)	C31—C32	1.381 (6)
C11—H11	0.9300	C31—S3	1.760 (4)
C12—C13	1.373 (8)	C32—C33	1.386 (7)
C12—H12	0.9300	C32—H32	0.9300
C13—C14	1.379 (7)	C33—C34	1.375 (10)
C13—H13	0.9300	C33—H33	0.9300
C14—H14	0.9300	C34—C35	1.366 (10)
C15—N2	1.485 (5)	C34—H34	0.9300
C15—H15A	0.9700	C35—C36	1.387 (7)
C15—H15B	0.9700	C35—H35	0.9300
C16—C21	1.373 (6)	C36—H36	0.9300
C16—C17	1.385 (6)	N1—S1	1.690 (3)
C16—S2	1.765 (4)	N2—S2	1.658 (3)
C17—C18	1.380 (7)	N3—S3	1.683 (3)
C17—H17	0.9300	O1—S1	1.417 (3)
C18—C19	1.370 (9)	O2—S1	1.426 (3)
C18—H18	0.9300	O3—S2	1.421 (3)
C19—C20	1.367 (9)	O4—S2	1.432 (3)
C19—H19	0.9300	O5—S3	1.416 (3)
C20—C21	1.364 (8)	O6—S3	1.420 (3)
C20—H20	0.9300		
C6—C1—C2	122.1 (4)	H22A—C22—H22B	107.7
C6—C1—N1	108.6 (3)	C24—C23—N3	107.8 (3)
C2—C1—N1	129.2 (4)	C24—C23—C22	127.3 (3)

C3—C2—C1	116.3 (6)	N3—C23—C22	124.9 (3)
C3—C2—H2	121.8	C23—C24—C25	110.0 (3)
C1—C2—H2	121.8	C23—C24—Br1	126.0 (3)
C4—C3—C2	122.5 (5)	C25—C24—Br1	123.7 (3)
C4—C3—H3	118.7	C30—C25—C26	120.0 (4)
C2—C3—H3	118.7	C30—C25—C24	107.0 (3)
C3—C4—C5	121.3 (5)	C26—C25—C24	132.9 (4)
C3—C4—H4	119.4	C27—C26—C25	117.5 (5)
C5—C4—H4	119.4	C27—C26—H26	121.2
C4—C5—C6	117.7 (6)	C25—C26—H26	121.2
C4—C5—H5	121.1	C28—C27—C26	121.6 (5)
C6—C5—H5	121.1	C28—C27—H27	119.2
C1—C6—C5	120.1 (4)	C26—C27—H27	119.2
C1—C6—C7	106.2 (3)	C29—C28—C27	122.3 (5)
C5—C6—C7	133.6 (5)	C29—C28—H28	118.8
C8—C7—C6	110.4 (4)	C27—C28—H28	118.8
C8—C7—Br2	127.2 (3)	C28—C29—C30	116.9 (5)
C6—C7—Br2	122.3 (3)	C28—C29—H29	121.6
C7—C8—N1	107.9 (3)	C30—C29—H29	121.6
C7—C8—C15	130.4 (3)	C25—C30—C29	121.6 (4)
N1—C8—C15	121.1 (3)	C25—C30—N3	107.9 (3)
C14—C9—C10	121.0 (4)	C29—C30—N3	130.3 (4)
C14—C9—S1	119.2 (3)	C36—C31—C32	122.1 (4)
C10—C9—S1	119.8 (3)	C36—C31—S3	119.1 (3)
C11—C10—C9	119.0 (5)	C32—C31—S3	118.8 (3)
C11—C10—H10	120.5	C31—C32—C33	118.3 (5)
C9—C10—H10	120.5	C31—C32—H32	120.9
C12—C11—C10	120.4 (5)	C33—C32—H32	120.9
C12—C11—H11	119.8	C34—C33—C32	119.6 (6)
C10—C11—H11	119.8	C34—C33—H33	120.2
C11—C12—C13	120.6 (5)	C32—C33—H33	120.2
C11—C12—H12	119.7	C35—C34—C33	121.6 (5)
C13—C12—H12	119.7	C35—C34—H34	119.2
C12—C13—C14	120.3 (5)	C33—C34—H34	119.2
C12—C13—H13	119.8	C34—C35—C36	119.2 (6)
C14—C13—H13	119.8	C34—C35—H35	120.4
C9—C14—C13	118.8 (4)	C36—C35—H35	120.4
C9—C14—H14	120.6	C31—C36—C35	119.2 (5)
C13—C14—H14	120.6	C31—C36—H36	120.4
N2—C15—C8	112.6 (3)	C35—C36—H36	120.4
N2—C15—H15A	109.1	C8—N1—C1	106.8 (3)
C8—C15—H15A	109.1	C8—N1—S1	121.4 (2)
N2—C15—H15B	109.1	C1—N1—S1	118.4 (3)
C8—C15—H15B	109.1	C15—N2—C22	115.8 (3)
H15A—C15—H15B	107.8	C15—N2—S2	113.9 (2)
C21—C16—C17	120.6 (4)	C22—N2—S2	112.5 (2)
C21—C16—S2	120.0 (3)	C30—N3—C23	107.2 (3)
C17—C16—S2	119.2 (3)	C30—N3—S3	120.8 (2)

C18—C17—C16	119.3 (5)	C23—N3—S3	121.9 (2)
C18—C17—H17	120.4	O1—S1—O2	119.9 (2)
C16—C17—H17	120.4	O1—S1—N1	105.65 (19)
C19—C18—C17	119.7 (5)	O2—S1—N1	107.17 (16)
C19—C18—H18	120.1	O1—S1—C9	109.3 (2)
C17—C18—H18	120.1	O2—S1—C9	109.17 (18)
C20—C19—C18	120.3 (5)	N1—S1—C9	104.47 (17)
C20—C19—H19	119.8	O3—S2—O4	120.0 (2)
C18—C19—H19	119.8	O3—S2—N2	106.90 (17)
C21—C20—C19	120.8 (5)	O4—S2—N2	106.97 (18)
C21—C20—H20	119.6	O3—S2—C16	109.1 (2)
C19—C20—H20	119.6	O4—S2—C16	107.72 (19)
C20—C21—C16	119.3 (5)	N2—S2—C16	105.13 (17)
C20—C21—H21	120.4	O5—S3—O6	120.34 (19)
C16—C21—H21	120.4	O5—S3—N3	105.89 (16)
C23—C22—N2	113.7 (3)	O6—S3—N3	107.18 (17)
C23—C22—H22A	108.8	O5—S3—C31	109.42 (18)
N2—C22—H22A	108.8	O6—S3—C31	108.5 (2)
C23—C22—H22B	108.8	N3—S3—C31	104.31 (17)
N2—C22—H22B	108.8		
C6—C1—C2—C3	1.0 (6)	C32—C33—C34—C35	-0.7 (9)
N1—C1—C2—C3	-176.3 (4)	C33—C34—C35—C36	2.2 (9)
C1—C2—C3—C4	-0.3 (8)	C32—C31—C36—C35	-0.6 (7)
C2—C3—C4—C5	0.3 (9)	S3—C31—C36—C35	-179.4 (4)
C3—C4—C5—C6	-0.9 (8)	C34—C35—C36—C31	-1.6 (8)
C2—C1—C6—C5	-1.7 (6)	C7—C8—N1—C1	1.3 (4)
N1—C1—C6—C5	176.1 (3)	C15—C8—N1—C1	-170.3 (3)
C2—C1—C6—C7	-178.1 (4)	C7—C8—N1—S1	-138.7 (3)
N1—C1—C6—C7	-0.4 (4)	C15—C8—N1—S1	49.7 (4)
C4—C5—C6—C1	1.6 (6)	C6—C1—N1—C8	-0.5 (4)
C4—C5—C6—C7	176.9 (4)	C2—C1—N1—C8	177.0 (4)
C1—C6—C7—C8	1.2 (4)	C6—C1—N1—S1	140.9 (3)
C5—C6—C7—C8	-174.6 (4)	C2—C1—N1—S1	-41.6 (5)
C1—C6—C7—Br2	179.2 (3)	C8—C15—N2—C22	-80.9 (4)
C5—C6—C7—Br2	3.4 (6)	C8—C15—N2—S2	146.3 (3)
C6—C7—C8—N1	-1.6 (4)	C23—C22—N2—C15	55.1 (4)
Br2—C7—C8—N1	-179.4 (3)	C23—C22—N2—S2	-171.5 (3)
C6—C7—C8—C15	169.0 (4)	C25—C30—N3—C23	0.3 (4)
Br2—C7—C8—C15	-8.8 (6)	C29—C30—N3—C23	176.2 (4)
C14—C9—C10—C11	0.2 (6)	C25—C30—N3—S3	146.3 (3)
S1—C9—C10—C11	-179.8 (3)	C29—C30—N3—S3	-37.7 (5)
C9—C10—C11—C12	-0.4 (7)	C24—C23—N3—C30	0.2 (4)
C10—C11—C12—C13	0.2 (8)	C22—C23—N3—C30	-176.6 (3)
C11—C12—C13—C14	0.2 (8)	C24—C23—N3—S3	-145.4 (3)
C10—C9—C14—C13	0.2 (6)	C22—C23—N3—S3	37.8 (5)
S1—C9—C14—C13	-179.8 (3)	C8—N1—S1—O1	-168.6 (3)
C12—C13—C14—C9	-0.5 (7)	C1—N1—S1—O1	55.9 (3)

C7—C8—C15—N2	-41.2 (5)	C8—N1—S1—O2	-39.6 (3)
N1—C8—C15—N2	128.3 (3)	C1—N1—S1—O2	-175.2 (3)
C21—C16—C17—C18	0.7 (7)	C8—N1—S1—C9	76.1 (3)
S2—C16—C17—C18	-173.8 (4)	C1—N1—S1—C9	-59.4 (3)
C16—C17—C18—C19	0.4 (8)	C14—C9—S1—O1	163.0 (3)
C17—C18—C19—C20	-1.0 (9)	C10—C9—S1—O1	-17.0 (4)
C18—C19—C20—C21	0.5 (10)	C14—C9—S1—O2	30.0 (4)
C19—C20—C21—C16	0.6 (9)	C10—C9—S1—O2	-150.0 (3)
C17—C16—C21—C20	-1.2 (7)	C14—C9—S1—N1	-84.3 (3)
S2—C16—C21—C20	173.2 (4)	C10—C9—S1—N1	95.7 (3)
N2—C22—C23—C24	-103.1 (4)	C15—N2—S2—O3	-45.1 (3)
N2—C22—C23—N3	73.1 (5)	C22—N2—S2—O3	-179.5 (3)
N3—C23—C24—C25	-0.6 (4)	C15—N2—S2—O4	-174.9 (3)
C22—C23—C24—C25	176.1 (3)	C22—N2—S2—O4	50.7 (3)
N3—C23—C24—Br1	-174.8 (3)	C15—N2—S2—C16	70.8 (3)
C22—C23—C24—Br1	1.9 (6)	C22—N2—S2—C16	-63.6 (3)
C23—C24—C25—C30	0.7 (4)	C21—C16—S2—O3	39.1 (4)
Br1—C24—C25—C30	175.1 (3)	C17—C16—S2—O3	-146.4 (3)
C23—C24—C25—C26	-176.4 (4)	C21—C16—S2—O4	170.9 (4)
Br1—C24—C25—C26	-2.0 (6)	C17—C16—S2—O4	-14.6 (4)
C30—C25—C26—C27	0.3 (6)	C21—C16—S2—N2	-75.3 (4)
C24—C25—C26—C27	177.2 (4)	C17—C16—S2—N2	99.2 (4)
C25—C26—C27—C28	-0.1 (7)	C30—N3—S3—O5	40.2 (3)
C26—C27—C28—C29	-1.0 (8)	C23—N3—S3—O5	-178.7 (3)
C27—C28—C29—C30	1.8 (7)	C30—N3—S3—O6	169.8 (3)
C26—C25—C30—C29	0.6 (6)	C23—N3—S3—O6	-49.1 (3)
C24—C25—C30—C29	-177.0 (4)	C30—N3—S3—C31	-75.2 (3)
C26—C25—C30—N3	177.0 (3)	C23—N3—S3—C31	65.8 (3)
C24—C25—C30—N3	-0.6 (4)	C36—C31—S3—O5	134.2 (3)
C28—C29—C30—C25	-1.6 (6)	C32—C31—S3—O5	-44.7 (4)
C28—C29—C30—N3	-177.1 (4)	C36—C31—S3—O6	1.1 (4)
C36—C31—C32—C33	2.0 (7)	C32—C31—S3—O6	-177.8 (3)
S3—C31—C32—C33	-179.1 (4)	C36—C31—S3—N3	-112.9 (3)
C31—C32—C33—C34	-1.4 (8)	C32—C31—S3—N3	68.2 (4)

Hydrogen-bond geometry (\AA , $^\circ$)

$D-H\cdots A$	$D-H$	$H\cdots A$	$D\cdots A$	$D-H\cdots A$
C2—H2 \cdots O1	0.93	2.43	2.993 (7)	119
C13—H13 \cdots O3 ⁱ	0.93	2.80	3.324 (6)	117
C14—H14 \cdots O4 ⁱ	0.93	2.78	3.558 (5)	142
C15—H15B \cdots O2	0.97	2.25	2.850 (5)	119
C18—H18 \cdots O3 ⁱⁱ	0.93	2.73	3.575 (6)	151
C19—H19 \cdots O4 ⁱⁱⁱ	0.93	2.59	3.443 (6)	152
C19—H19 \cdots O6 ⁱⁱⁱ	0.93	2.81	3.467 (6)	129
C20—H20 \cdots Br2 ⁱⁱⁱ	0.93	3.02	3.536 (5)	117
C22—H22A \cdots O6	0.97	2.39	2.950 (5)	116
C27—H27 \cdots O1 ^{iv}	0.93	2.48	3.389 (6)	164

C28—H28···O5 ^v	0.93	2.63	3.547 (6)	170
C29—H29···O5	0.93	2.35	2.907 (5)	118
C34—H34···O5 ⁱⁱ	0.93	2.62	3.360 (6)	137
C35—H35···Cg(C16—C21) ^{vi}	0.93	2.91	3.729 (7)	147

Symmetry codes: (i) $x-1/2, -y+1/2, z-1/2$; (ii) $x+1, y, z$; (iii) $x+1/2, -y+1/2, z-1/2$; (iv) $-x+1, -y+1, -z+1$; (v) $-x+1, -y+1, -z+2$; (vi) $x-1/2, -y-1/2, z-1/2$.